AGU100 ADVANCING EARTH AND SPACE SCIENCE

JGR

Journal of Geophysical Research: Atmospheres

RESEARCH ARTICLE

10.1029/2018JD028536

Key Points:
- CCLM model results were evaluated in terms of agricultural indices for cropping of maize, sorghum, and pearl millet across three different agroecological zones in West Africa
- High-resolution future climate projections indicate a shortening of the rainy seasons by approximately 2 weeks in the Sahel region till the end of the century
- The projected decreases (increases) of rainfall (temperature) over the Sahel region would negatively impact on water availability (WAV) and growing degree days (GDD)

Supporting Information:
- Figures S1 and S2

Correspondence to:
D. Dieng,
diarra.dieng@partner.kit.edu

Citation:
Dieng D. B., Laux, P., Smiatek, G., Heinzeller, D., Bliefernicht, J., Kunstmann, H. G., et al. (2018). Performance analysis and projected changes of agroclimatological indices across West Africa based on high-resolution regional climate model simulations. *Journal of Geophysical Research: Atmospheres*, *123*, 7950–7973. https://doi.org/10.1029/2018JD028536

Received 15 FEB 2018
Accepted 30 JUN 2018
Accepted article online 11 JUL 2018
Published online 12 AUG 2018

Performance Analysis and Projected Changes of Agroclimatological Indices Across West Africa Based on High-Resolution Regional Climate Model Simulations

Diarra Dieng[1,2,3], Patrick Laux[1,2], Gerhard Smiatek[2], Dominikus Heinzeller[1,4], Jan Bliefernicht[2], Abdoulaye Sarr[5], Amadou Thierno Gaye[3], and Harald Kunstmann[1,2]

[1]Institute of Meteorology and Climate Research (IMK-IFU), Campus Alpine, Karlsruhe Institute of Technology (KIT), Karlsruhe, Germany, [2]Institute of Geography, University of Augsburg, Augsburg, Germany, [3]Laboratoire de Physique de l'Atmosphere et de l'Ocean Siméon Fongang (LPAO-SF), Ecole Supérieure Polytechnique, Université Cheikh Anta Diop, Dakar-Fann, Senegal, [4]Cooperative Institute for Research in Environmental Sciences, NOAA/OAR/ESRL/Global Systems Division, University of Colorado Boulder, Boulder, CO, USA, [5]Agence nationale de l'Aviation civile et de la Météorologie, Dakar, Senegal

Abstract In this study, we analyze a set of agroclimatological indices across West Africa and assess their projected changes for the future. We apply the regional climate model CCLM (COnsortium for Small-scale MOdelling in CLimate Mode) with a high spatial resolution of 0.11° (approximately 12 km) under current (1981–2010) and future climate conditions, based on the emission scenario RCP4.5. The focus is on purely rainfall-based indices, that is, the onset (ORS), the cessation (CRS), and the length of the rainy season (LRS) and the joint rainfall- and temperature-based indices, that is, growing degree days (GDD) and the water availability (WAV), derived for maize, sorghum, and pearl millet across Guinea, Savanna, and Sahel. For the present, in general, the CCLM compares well to observations, represented by three different products. However, CCLM shows limitations in the representation of the CRS over Guinea with a delay of >30 days and the GDD and WAV over Sahel with biases up to 30% and 70% for all crops. For the future climate projections, ORS, CRS, and LRS are expected to be delayed up to 2 weeks for most regions, in particular for the period 2071–2100. The GDD is expected to increase by around 8% till 2021–2050 and by around 5% till 2071–2100 for all crops. The WAV is expected to be decreased by up to 10% in 2021–2050, and by up to 24% in 2071–2100 in Sahel, and <12% over Guinea and Savanna in both periods. In particular, we evaluate the added value of the high-resolution CCLM information for decision support in agricultural management.

1. Introduction

It has been estimated that the annual world production of crops and livestock will need to be 60% higher in 2050 than in 2006 (FAO [Food and Agriculture Organization], 2016) in order to meet the demand for food. In particular for West Africa, the population is expected to increase significantly by about 54% in 2050 and about by 82% in 2100 (United Nations Population Division [UN], 2017). At the same time, negative crop yield trends are predicted for the forthcoming decades for most of the staple crops (Lobell et al., 2008).

West Africa is mainly characterized by rainfed agriculture and is thus highly vulnerable to climate change. Due to the growing competition for water and the high investment costs in irrigation development, further expansion of irrigation across West Africa remains unlikely. Rainfall is already highly variable under current conditions, and the variability is expected to increase further under climate change.

Apart from severe droughts, it is mainly the intraseasonal and the interannual rainfall variability, which may cause crop failure and food shortages (e.g., Mishra et al., 2008; Sivakumar, 1988; Sultan et al., 2005; Syed et al., 2010). For instance, Wheeler et al. (2007) simulated the effect of evenly and unevenly distributed intraannual rainfall on crop yield, independently of the total seasonal rainfall amount. For this reason, the success of planting depends on the knowledge of the agricultural onset of the rainy season (subsequently referred to as ORS). The ORS coincides with the planting date, which belongs to the most crucial tactical decisions under rainfed agriculture, especially in semiarid regions where the rainy season is limited to a few months per year only. Planting too early might lead to crop failure in case no significant rain will fall within days thereafter.

Conversely, planting too late may reduce valuable growing time and hinder the crop of reaching maturity. Salack et al. (2011) showed that the onset of the rainy season is often followed by dry spells, known as “false starts” of the wet season in literature.

In order to study the onset of the rainy season, it is important to distinguish between two general approaches, one for large-scale meteorological and the other for local-scale agricultural applications (Vellinga et al., 2013). For agricultural applications, an accurate prediction of the date of the ORS is more useful than a good prediction of total rainfall. For this reason, a number of rainfall threshold-based approaches have been developed to predict the agriculturally relevant ORS in West Africa. One of the commonly used rainfall threshold-based approaches is the definition of Stern et al. (1981), which states that the wet season has started when, for the first time after 1 March, 25 mm of rain are being exceeded within two consecutive days, and no dry period of 10 or more days occurs in the following 30 days. Prior to its application, however, the user is asked to adapt these criteria, which strongly depend on local weather conditions, soil types, the evaporative demands of crops, and cropping practices. Consequently, a wide variety of derivatives of this definition exists for West Africa (e.g., Morel, 1992; Omotosho, 1990; Sivakumar et al., 1993; Traoré et al., 2000).

Laux et al.(2008, 2009) extended the definition of Stern et al. (1981) for the Volta basin of West Africa by using a fuzzy logic approach. The major advantage of this extension is that the ORS does not strictly depend on fixed rainfall thresholds. As an example, it should not make any difference for planting if 25 mm or only 24.9 mm of rainfall. In a series of follow-up studies, rainfall thresholds have been optimized for specific regions by coupling this fuzzy logic ORS approach to process-based crop models (Laux et al., 2010; Waongo et al., 2014, 2015). Similarly, threshold-based approaches for the cessation of the rainy season (CRS) have been developed. Mugalavai et al. (2008), Oladipo and Kyari (1993), and Sivakumar (1988) investigated the fluctuations in the ORS, the CRS, and the length of the rainy season (LRS) in West Africa. They reported a poor performance on determining the CRS, which results also in poor estimates of the LRS.

Also, simpler approaches based on the (annual) cumulative rainfall amounts are in use to determine the ORS and the CRS. Examples are presented by Olaniran (1983) and Odekunle (2004, 2006). Besides the ORS, CRS, and LRS, further measures are of interest in agriculture. One crucial measure is the growing degree day (GDD), which can be used to assess the suitability of a region for production of a particular crop (Carew et al., 2009), to estimate the growth stages of crops (Miller et al., 2001), maturity, and harvesting (Parthasarathi et al., 2013) and to predict best timing of fertilizer or pesticide applications (Herms, 2004; Juszczak et al., 2008). Many studies applied the aforementioned ORS approaches (precipitation threshold-based and cumulative sum approaches) in combination with observed rainfall series but rarely in combination with output from regional climate models (RCMs). Modeling studies by Ramel et al. (2006), Sijikumar et al. (2006), and Vanvyve et al. (2008) have used individual coarse-resolution climate models to simulate the monsoon onset. They found that models are useful to expose processes related to the African monsoon onset. Recently, within the framework of the Coordinated Regional Downscaling Experiment project, Mounkaila et al. (2015) evaluated nine RCMs in simulating the rainfall onset dates. They concluded that the RCMs ability in simulating ORS depends strongly on the models capability in simulating the monsoon system features and on the definition of the ORS. Kim et al. (2008) pointed out that the models with high resolutions generally reproduce better spatial patterns of monsoon precipitation compared to models with lower resolution. Therefore, based on these conclusions, we performed our new very high-resolution regional climate simulations.

In this study, the value of high-resolution RCM simulations is assessed for agricultural management. The high-resolution simulations were performed using CCLM (COnsortium for Small-scale MOdelling in CLimate Mode; Doms et al., 2011) based on the configuration presented in Dieng et al. (2017). Agroclimatological parameters are derived for the past (1981–2010) and two future periods (2021–2050 and 2071–2100), comprising ORS, CRS, and LRS, as well as GDD and water availability (WAV). More specifically, we applied two conceptually different ORS and CRS approaches, that is, a threshold-based and a cumulative approach to the results of the high-resolution CCLM climate projections across West Africa. The ORS and CRS are not specific for the different crops, but GDD and WAV are specifically calculated for cropping of maize, sorghum, and pearl millet.

The present study is structured as follows: In section 2, we describe the setup of the experiment including the RCM, the study regions, the selected crops, and the definition of the agroclimatological indices. In section 3, we evaluate the RCM for the present climate and discuss the simulated future changes of the investigated indicators. Conclusions are drawn in section 4.

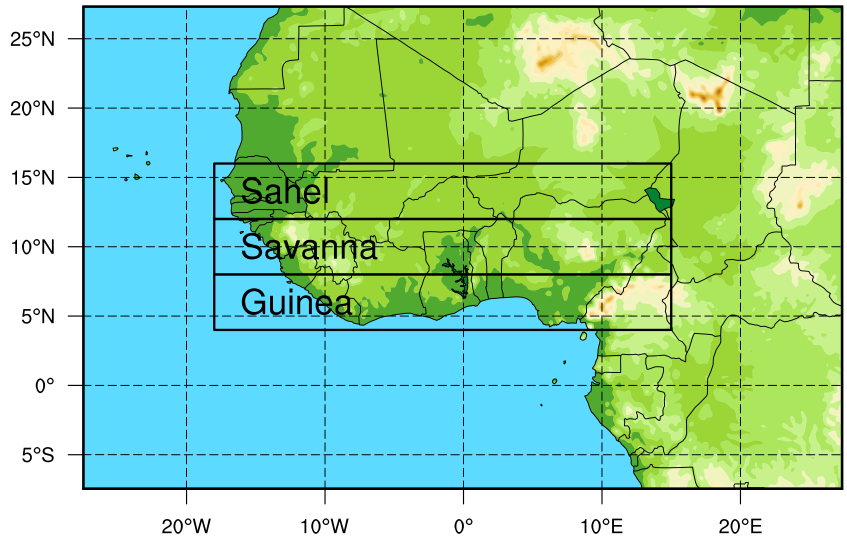

Figure 1. Model domain and delineation of the three different agroclimatic zones: Guinea, Savanna, and Sahel, following Omotosho and Abiodun (2007), Abiodun et al. (2012), and Mounkaila et al. (2015).

2. Material and Methods

2.1. Setup of the RCM CCLM

The simulations analyzed in this study were performed using the CCLM RCM (version 4.8), driven by the lateral boundary conditions from the MPI-LR (ECHAM6) global Earth System Model (Stevens et al., 2013). The climate simulations are based on the RCP4.5 emission scenario. For the downscaling, a nested approach has been used applying two domains at 0.44° (50 km) and 0.11° (12 km) resolution. More details about the CCLM setup and an evaluation of a simulation driven with ERA-Interim reanalysis data are given in Dieng et al. (2017). The authors concluded that CCLM is able to reproduce the major observed climate characteristics across West Africa, including the West African Monsoon (WAM). However, CCLM exhibited shortcomings in the simulation of the WAM. The progression of the WAM tended to be too far to the north, leading to a significant overestimation of the precipitation amount by 60% during June, July, August, and September in the Sahel region. On the other hand, the precipitation amount over the Guinea region was underestimated. In general, a lower precipitation bias was obtained in the high-resolution (0.11°) simulations. For this reason, this study is restricted to the CCLM simulation in 0.11° exclusively. The evaluation is performed with ECHAM6 for the present-day climate (1981–2010), and we discuss the expected future climate change impact for the two future 30-year periods, from 2021 to 2050 (near future) and from 2071 to 2100 (far future). The evaluation is restricted to over land only. All applied observational reference data sets were resampled to 0.11° resolution. For computational and storage reasons, we limited our study to one scenario (i.e., RCP4.5), in favor for this high spatial resolution.

2.2. Study Region

The model evaluation and the assessment of the expected future climate change impact are performed for three different regions with different climatic characteristics. The differentiation is related to the precipitation amount and length of the rainy season but also linked to agroecological features. These areas are Guinea (4°N to 8°N), Savanna (8°N to 12°N), and Sahel (12°N to 16°N; Figure 1). The west-east extension of the study region is from 18°W to 15° E following previous studies (Abiodun et al., 2012; Mounkaila et al., 2015; Omotosho & Abiodun, 2007). Similar regions were also used for an identification of the spatiotemporal evolution of the agroclimatical risks for Benin, Togo, and Nigeria (Alhassane et al., 2013), for an assessment of the impact of climate change on the yield of sorghum and millet (Sultan et al., 2013), and for the improvement of the risk assessment related to historical trends in temperature and rainfall variability on crop water demand, biomass, and grain yields of pearl millet and maize (Salack et al., 2015).

2.3. Validation Data

This study uses a set of climate reference data, providing information on daily rainfall amount as well as mean, maximum, and minimum temperature. These data sets include AgMERRA (Agricultural Modern-Era Retrospective Analysis for Research and Applications; Ruane et al., 2015), CHIRPS (Climate Hazards Group

Table 1
Several Temperature and Rainfall Characteristics for Different Plant Growth Phases of the Selected Crops Used in This Study

Characteristics	Crops: Maize	Sorghum	Pearl millet
	Phase 1 (germination and emergence to leaf development)		
Days after sowing (days)	5–55	0–30	0–21
T_{mean} (°C)	26–35	20–36	25–36
T_{opt} (°C)	19	25	10
T_{max} (°C)	>26	>35	>25
Max. water (mm)	50–200	150	50
	Phase 2 (flowering and grain development)		
Days after sowing (days)	57–120	21–42	21–42
T_{mean} (°C)	21–30	26–34	23–32
T_{opt} (°C)	22	20	21
T_{max} (°C)	35	<33	<35
Max. water (mm)	>150–250	<150	150
	Phase 3 (grain filling, ripening, and physiological maturity)		
Days after sowing (days)	102–140	65–110	42–77
T_{mean} (°C)	21–30	23–31	22–32
T_{opt} (°C)	25	24	<33
T_{max} (°C)	<45	>35	42
Max. water (mm)	<50	50	<200
Min. water (mm/year)	600–1,200	500–1,000	400–900
Planting date	May/June	March/April	March/April
Critical stages	Phase 3	Phase 2	Phase 2
T_{crit} (°C)	35	40	45
T_{base} (°C)	10	25	23

Infrared Precipitation with Stations; Funk et al., 2014), UDEL (University of Delaware; Willmott & Matsuura, 1995), and EWEMBI. This acronym is built from **E**2OBS (EartH2Observe forcing data; Calton et al., 2016) and **W**FDEI (WATCH Forcing Data methodology; Weedon et al., 2014) applied to **E**RA-Interim data (Dee et al., 2011) **M**erged and **B**ias-corrected for **I**SIMIP (Inter-Sectoral Impact Model Intercomparison Project). CHIRPS data have a spatial resolution of 0.05 × 0.05° and is available from 1981 onward to near present. AgMERRA and EWEMBI are at 0.5 × 0.5° resolution and cover the entire globe and a period from 1980 to 2010 and 1979 to 2013, respectively.

2.4. Selected Crops and Considered Agricultural Indices

The main staple crops of the regions are maize, sorghum, and pearl millet. According to USAID and FAO, maize contributes with about 20%, sorghum with 22%, and millets (pearl and finger) with 19% to domestic food production (FAO Statistics Division 2015). The model evaluation and the assessment (Table 1). During the growing season, the minimum water requirement is 500–600 mm for maize and 400 mm for sorghum. In comparison to the others crops, pearl millet is more suitable for hot and dry climates. It can even be grown in areas, where rainfall does not exceed 300 mm. However, during particular growth stages, wet conditions may also be harmful for the crops.

In addition to precipitation, temperature is the second major environmental factor affecting the growth, development, and yield of crops. The favorable or optimal day and night temperature range for plant growth and maximum yields varies among the crop species. The life cycle of crops is characterized by the base temperature T_{base} and the optimum temperature T_{opt} requirement to complete a specific phenophase or, if integrated, the whole life cycle. Besides daily average temperature (T_{mean}), also maximum temperature (T_{max}) must be considered. Several studies found that temperatures of above 35°C are lethal to maize pollen

10.1029/2018JD028536

Table 2
Temperature- and Precipitation-Related Agroclimatological Indices Used in This Study

Acronym	Description	Unit
MST	Mean seasonal temperature	°C
MSP	Mean seasonal precipitation	mm
ORS	Onset of rainy reason	days
	DEF1: first day of a pentad starting from 1 March with more than one wet day, in which more than 15 mm of rainfall fall and which is not followed by a dry spell >6 days within the next 30 days after the planting. A wet day is defined as a day with precipitation >1 mm (Laux et al., 2008).	
	DEF2: 8% of the annual cumulative rainfall within 5-day spell (Ilesanmi, 1972; Odekunle, 2004)	
CRS	Cessation of rainy season	days
	DEF1: first date after September without a wet day in the following 20 days. A wet day is defined as a day with precipitation >1 mm (Laux et al., 2008).	
	DEF2: 90% of the annual cumulative rainfall within 5-day spell. (Ilesanmi, 1972; Odekunle, 2004)	
LRS	Length (duration) of rainy season	days
	DEF1 = DEF2 = CRS − ORS + 1	
GDD	Growing degree days	°C
WAV	Water availability	mm

viability (Dupuis & Dumas, 1990; Herrero & Johnson, 1980; Schoper 1987). Leaf photosynthesis rate of maize has a high T_{opt} of 33 to 38°C (Crafts-Brandner & Salvucci, 2002). Maiti et al. (1996) reported that sorghum vegetative growth has a T_{opt} of 26–34°C, while reproductive growth has a T_{opt} of 25–28°C. For example, the vegetative development of sorghum has a T_{base} of 8°C and a T_{opt} of 34°C (Alagarswamy & Ritchie, 1991), while reproductive development of sorghum has a T_{opt} of 31°C (Prasad et al., 2006). The temperature for the growth of pearl millet ranges from a base temperature of 10–12° C to a sharply defined optimum at 33–34°C and drops to 0 at about 45–47°C (Ong & Monteith, 1985).

Table 1 gives an overview of the selected crops with the difference stages of the growing cycle (phenophases), the approximate number of days, and temperature and rainfall requirements at the three major phases of development. Phase 1 corresponds to the vegetative phase; Phase 2, to the reproductive phase; and Phase 3, to the maturity stage. Table 1 summarizes temperature and rainfall characteristics for the plant growth phases, following the recommendations of United States Agency for International Development.

The applied indices were selected from an agroclimatological point of view, and the focus is set on a performance analysis for subsequent agroclimatological impact modeling. Acronyms and the applied statistics are listed in Table 2. For this study, we have used two definitions (DEF1 and DEF2) of the ORS and the CRS. The LRS for both definitions corresponds to the difference between the cessation and the onset. DEF1 is based on Laux et al. (2008); and DEF2, on Ilesanmi (1972) and Odekunle (2004). DEF1 is a threshold-based definition accounting for the rainfall amount, the number of rainy events, and the "false starts." Preliminary results reveal that thresholds between 15 and 25 mm falling within three consecutive days and no dry spell of >6 days within a period of 16 to 22 thereafter is appropriate for the domain of West Africa (Laux et al., 2008, 2009). The CRS is based on two threshold values, that is, the rainy day threshold and the number of consecutive dry days. Here 0.5 mm as threshold for a rainy day and 7 days for a dry spell period are selected for West Africa based on previous results (not shown). The onset and cessation dates in DEF2 are determined using the cumulative percentage mean rainfall constructed from 5-day rainfall averages (pentads).

The most common temperature index used to estimate complete crops growth and development is the GDD. The measure is calculated throughout the season for each planting date, given by

$$GDD = \sum_{i=PD}^{MVP} GD(i), \tag{1}$$

where *PD* is the planting date, *MVP* is the minimum vegetative period, and *GD*(*i*) is the daily accumulations of heat.

$$GD(i) = \begin{cases} 0 \quad \textit{if} \quad T(i) < T_{\text{base}} \quad \text{or} \quad T(i) > T_{\text{crit}}, \\ T(i) - T_{\text{base}} \quad \text{if} \quad T_{\text{base}} \le T(i) \le T(\text{crit}), \end{cases} \tag{2}$$

$$T(i) = (T_{\min}(i) + T_{\max}(i))/2. \tag{3}$$

Days that are warmer than normal may increase the plant growth (Miller et al., 2001), and each development stage requires a specific amount of accumulated GDD. Regarding the summer crops growing season, the FAO reports two different ranges of values. Maize requires a GDD between 100 and 120; sorghum, between 120 and 130; and pearl millet, between 80 and 120 days to reach maturity. The base temperatures T_{base} are determined experimentally and are different for the various crops. The reported base temperature for maize development is 10°C, while it is 25°C for sorghum and 23°C for pearl millet (Del Rio & Brent, 2014).

For maize, the GDD is set to 10 and 35°C for the lower and higher boundaries, respectively. To be specific, a day with a temperature below 10 and above 35°C does not contribute to increase the GDD, while a day with a temperature between 10 and 35°C does. Degree days are then summed over all 100 days in the growing season, which correspond to the minimum vegetative period of maize.

The WAV is the precipitation amount during the minimum vegetation period and amounts to 100 days for maize, 120 days for sorghum, and 80 days for pearl millet. This measure is calculated using the following equation:

$$WAV = \sum_{i=PD}^{MVP} RR(i), \tag{4}$$

where *RR*(*i*) corresponds to the daily rainfall amount.

3. Results

3.1. Evaluation of Present Climate and Agrometeorological Characteristics

Evaluating the 0.11° high-resolution regional climate runs shows that CCLM is in general capable of reasonably reproducing the observed regional- and local-scale mean temperature (1981–2010) features across West Africa (see supporting information Figure S1) for the seasons MAM (March–May) and JJA (June–August). However, based on the various observational data sets, the simulations exhibit distinct biases (calculated as model minus observation) of varying magnitudes for the different subregions. The spatial distribution of the biases based on the different observational data sets is shown in Figure 2. It can be seen that negative biases prevail across the West African domain. Although having different magnitudes for the different observational data sets, the spatial patterns of the biases are similar. Figure 3 depicts the distribution of the biases across the three agroecological zones as defined in Figure 1. It can be clearly seen that MAM simulations are closer to the observations. While the biases (magnitude and distribution) are comparable for AgMERRA and UDEL, the median of the bias distribution is significantly lower for EWEMBI, in particular for the Guinea and the Savanna regions. During MAM, the smallest biases in the mean temperature are found in the Savanna regions with less than 1°C. The biases in the Guinea and the Sahel regions in MAM and in all areas during JJA are larger and around approximately 2.1°C. There is an increasing range in the biases from south to north, following the observed temperature gradient (and variability). It should be noted that the mean difference between the observational data sets is up to 0.6°C. Overall, the spread in the bias distribution as well as the magnitude of the biases is largest for the Sahel region. This is in agreement with previous Coordinated Regional Downscaling Experiment regional climate studies (e.g., Dosio & Panitz, 2016; Dosio et al., 2015), which found similar temperature biases for the present climate in regions above 20°N.

The simulated precipitation patterns are in good agreement with the observations (see supporting information Figure S2), but the major band of precipitation (Intertropical Convergence Zone) is shifted further to the north in JJA. This causes a precipitation overestimation in the northern part of the Sahel region, similar to what was found for the CCLM simulation driven by the ERA-Interim reanalyses (Dieng et al., 2017). The simulated mean seasonal precipitation and the bias to the different observations is shown in Figure 4. The biases range

10.1029/2018JD028536

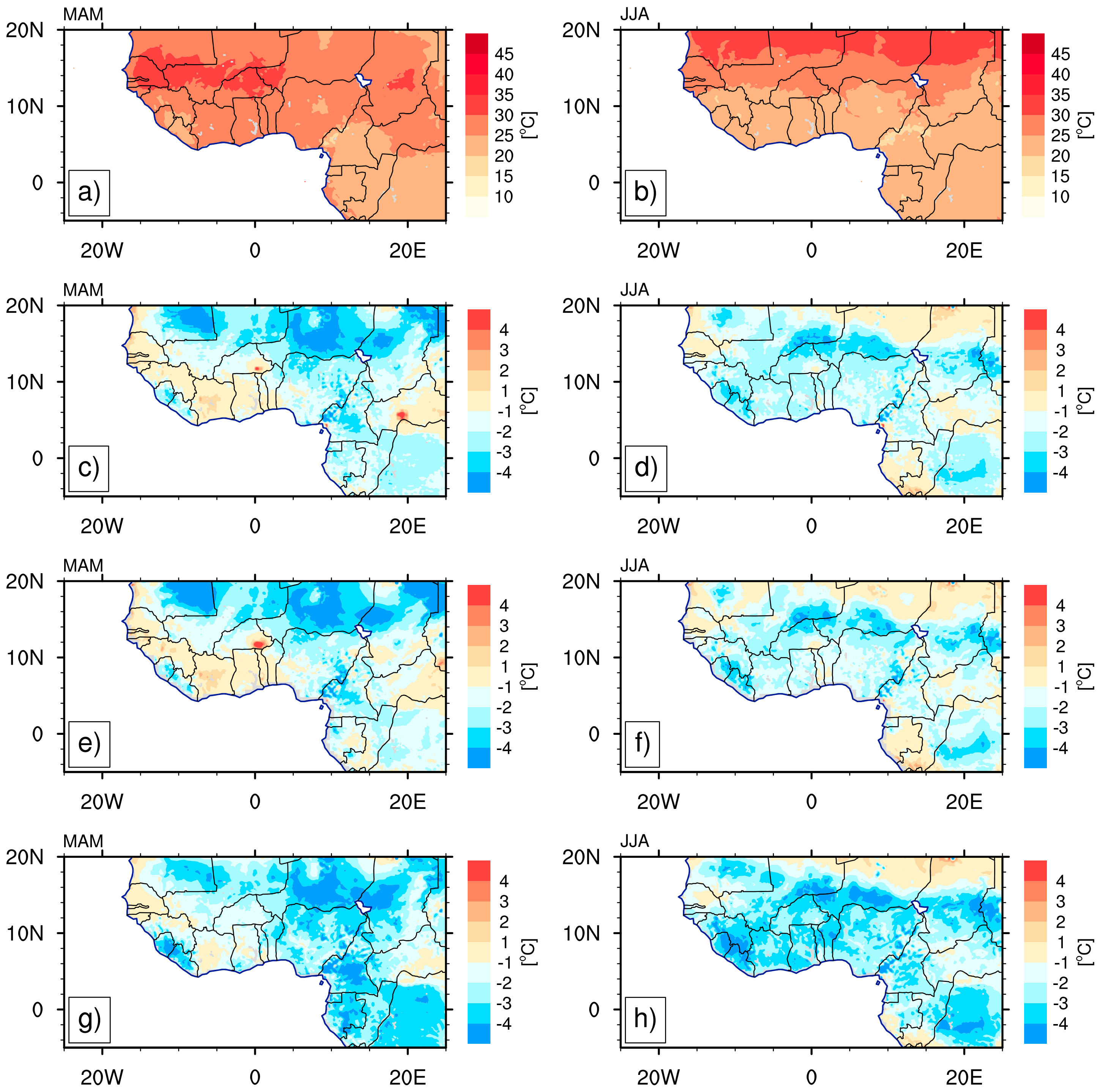

Figure 2. Simulated CCLM mean seasonal temperature in degrees Celsius for the period 1981–2010 (a, b). Biases related to the reference data sets AgMERRA (c, d), UDEL (e, f), and EWEMBI (g, h). Left panel depicts the MAM (March, April, and May) season, while the right panel depicts the JJA (June, July, and August) season. CCLM = COnsortium for Small-scale MOdelling in CLimate Mode; AgMERRA = Agricultural Modern-Era Retrospective Analysis for Research and Applications; UDEL = University of Delaware; EWEMBI = E2OBS and WFDEI applied to ERA-Interim data Merged and Bias-corrected for Inter-Sectoral Impact Model Intercomparison Project.

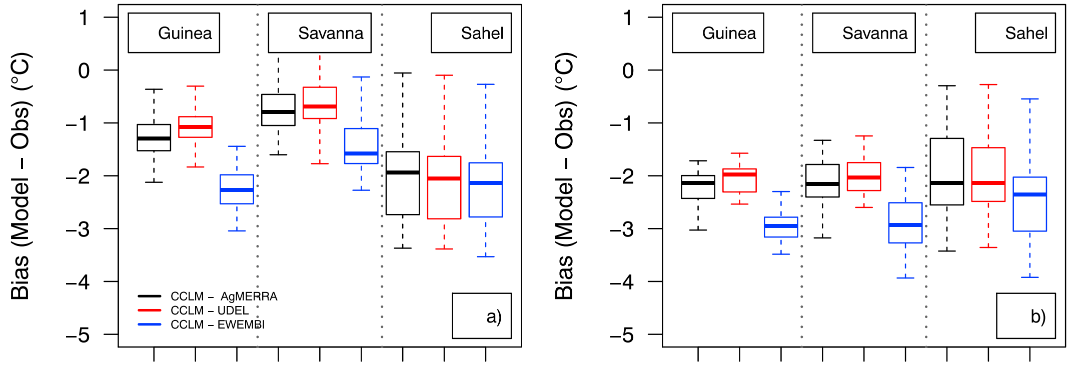

Figure 3. Areal bias (1981–2010) of the simulated CCLM temperature to the observations AgMERRA, CHIRPS, and EWEMBI for the season MAM (a) and season JJA (b) over the subregions Guinea, Savanna, and Sahel. MAM = March, April, and May; JJA = June, July, and August; CCLM = COnsortium for Small-scale MOdelling in CLimate Mode; AgMERRA = Agricultural Modern-Era Retrospective Analysis for Research and Applications; UDEL = University of Delaware; EWEMBI = E2OBS and WFDEI applied to ERA-Interim data Merged and Bias-corrected for Inter-Sectoral Impact Model Intercomparison Project.

from 5 mm in EWEMBI to 37 mm in AgMERRA during MAM and from 27 mm in EWEMBI to 55 mm in AgMERRA during JJA. Table 3 shows the relative precipitation biases for the three subregions. The biases in the Guinea region range from −8% to −15% and from 0.2% to 5.4% in the Savanna region and reach values up to 200% in the Sahel region during the MAM season. In JJA, there is a wet bias of around 20% in the Guinea region and around −2% and 4% in the Savanna region. In the Sahel region, the precipitation is overestimated by approximately 30%. Again, there is difference between the mean value in the observations ranging between −4.5% and 2.7% in the Guinea region, between −6% and 0.6% in the Savanna region, and between −11% and 22% in the Sahel region. Similar biases were reported by Sylla et al. (2015) and Diallo et al. (2016), who applied the RegCM4 model driven by ECHAM6.

After quantifying the temperature and precipitation biases across the three agroclimatic zones, selected agroclimatological indices for agricultural management are derived. The evaluation focuses on how well CCLM can estimate the mean dates of the ORS, the CRS, and the LRS for the period 1981–2010 using two different definitions. Afterward, the estimated CCLM GDD and WAV are compared to the values from AgMERRA, CHIRPS, and EWEMBI reference data.

3.2. Agroclimatological Indices

Figure 5 shows the calculated mean onset dates for CCLM and the different observation products by applying the definitions DEF1 and DEF2 (see section 2.4) for the period 1981–2010. The mean ORS dates follow the overall precipitation pattern (see supplementary Figure S2). They range between DOY (day of year) 50 to DOY 100 (21 February to 10 April) over the Guinea region, between DOY 100 and DOY 175 (10 April to 24 June) over the Savanna region, and between DOY 200 and DOY 250 (19 July to 8 September) over the Sahel region. The calculated mean ORS dates can differ significantly between DEF1 and DEF2, in particular for the Sahel region. This is in line with previous study over Burkina-Faso (Waongo et al., 2015), using DEF1 in combination with a process-based crop model to derive optimized planting dates. These authors derived similar dates that in general follow the prevailing north-south gradient of rainfall, raising strong evidence of location-specific ORS dates across West Africa. DEF1 and DEF2 correspond over the Guinea region, but the simulations produce a delay in the mean ORS (about 27 days) compared to the different observations for both definitions. On the other hand, CCLM is comparable to the observation products for both definitions over the Savanna region, while earlier mean ORS dates are simulated over the Sahel region, compared to the observations (Table 4). These differences are more pronounced in DEF1 (up to 60 days) than in DEF2 (up to 50 days). It has been shown, for example, by Stewart (1986) and Sivakumar (1998) that for bimodal rainfall regions such as the Guinea zone, the preferred crop type depends on the ORS. For an early start, maize can be grown, while a delayed onset favors sorghum and millet.

The variability in the ORS across West Africa is illustrated by its standard deviation. Figure 6 shows a homogeneous pattern of the standard deviation of ORS for DEF2 but a more scattered pattern for DEF1. For instance, a decreased standard deviation (around 10 days) for the region southerly of Senegal in the CCLM and the

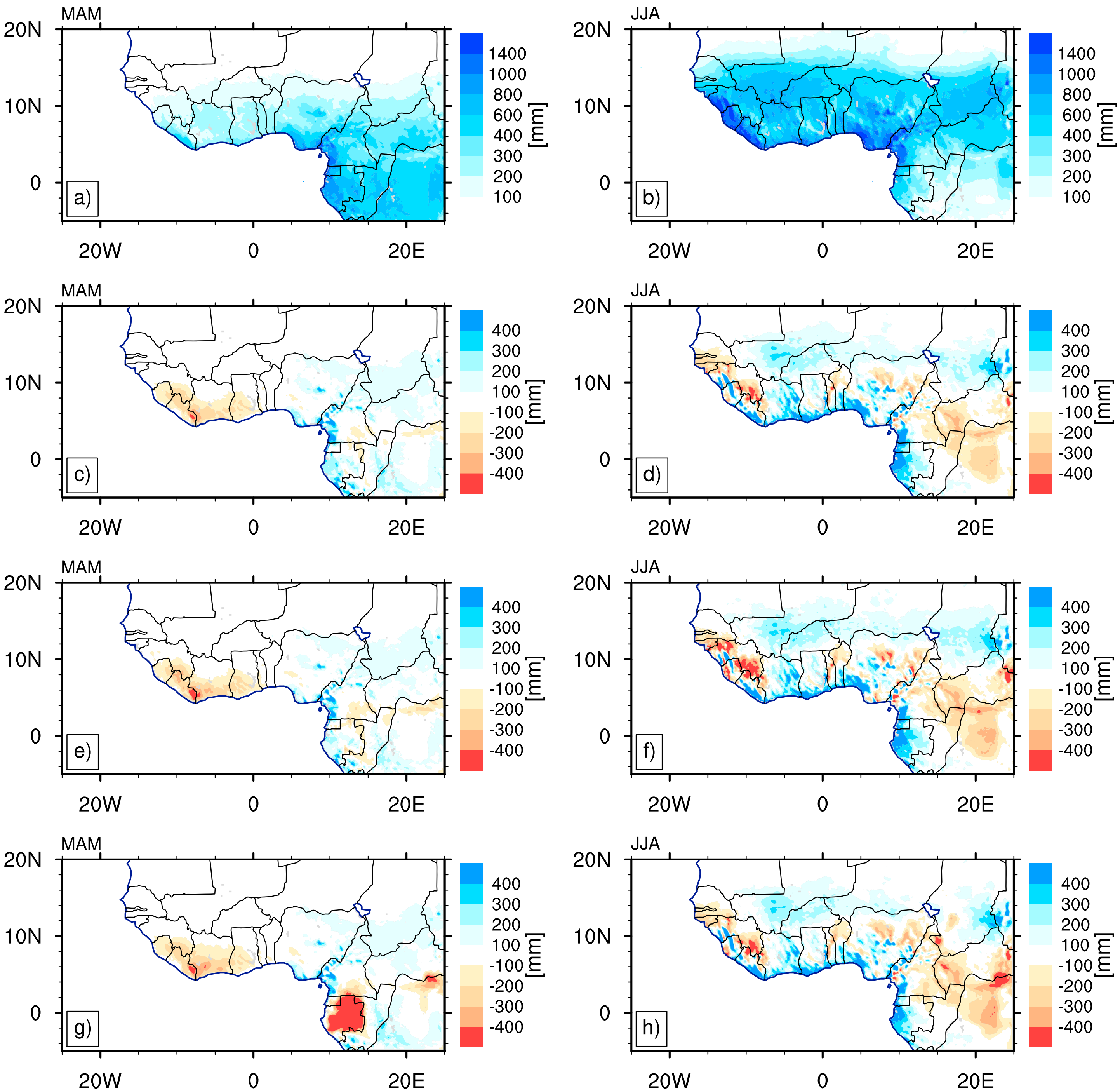

Figure 4. Simulated mean seasonal precipitation of COnsortium for Small-scale MOdelling in CLimate Mode (a, b) and bias to Agricultural Modern-Era Retrospective Analysis for Research and Applications (c, d), Climate Hazards Group Infrared Precipitation with Stations (e, f), and E2OBS and WFDEI applied to ERA-Interim data Merged and Bias-corrected for Inter-Sectoral Impact Model Intercomparison Project (g, h) in millimeters for the period 1981–2010. Left panel: season MAM (March–May) and right panel: season JJA (June–August).

observations compared to its surrounding is found. The results also show a lower standard deviation for DEF2 for most of the domain but a considerably increased value above 14°N in the CCLM for DEF1 as well as the observations for DEF2. The highest variability of ORS is found around 14–16°N for the simulations, probably due to the high variability of precipitation. In addition to the spatial representation in Figure 5, Figure 7 shows the probability density functions of the mean ORS dates over the three regions. A large dispersion between the observations is found for DEF1, in particular for the Guinea zone. This result is in agreement with the annual

10.1029/2018JD028536

Table 3
Observed AgMERRA, CHIRPS, and EWEMBI Area Mean Precipitation (mm) and Bias of the CCLM Simulation (%) Over Guinea, Savanna, and Sahel Investigation Areas for the Period 1981–2010

	MAM						JJA					
	Guinea		Savanna		Sahel		Guinea		Savanna		Sahel	
Index	(mm)	(%)	(mm)	(%)	(mm)	(%)	(mm)	(%)	(mm)	(%)	(mm)	(%)
AgMERRA	407	−10.4	191	5.4	27.2	153	655	20.3	655	3.4	366	29.7
CHIRPS	427	−14.6	195	3.6	22.9	200	694	18.4	689	−1.8	356	33.4
EWEMBI	428	−14.8	201	0.2	27.8	148	686	19.7	700	−3.3	382	24.2

Note. AgMERRA = Agricultural Modern-Era Retrospective Analysis for Research and Applications; CHIRPS = Climate Hazards Group Infrared Precipitation with Stations; EWEMBI = E2OBS and WFDEI applied to ERA-Interim data Merged and Bias-corrected for Inter-Sectoral Impact Model Intercomparison Project; CCLM = COnsortium for Small-scale MOdelling in CLimate Mode; JJA = June–August; MAM = March–May.

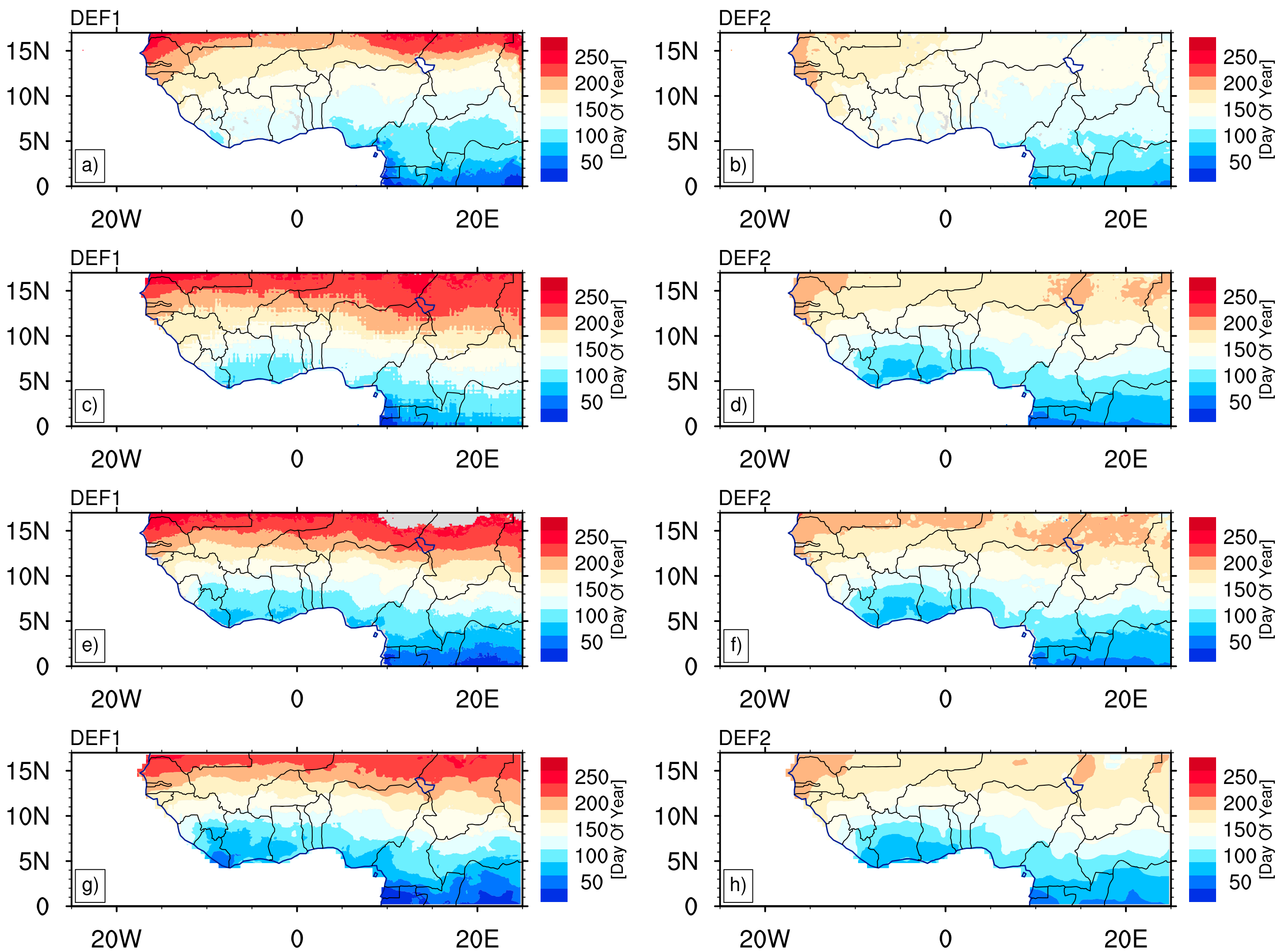

Figure 5. Mean onset date (ORS) for the period 1981–2010 according to definition DEF1 (left panel) and DEF2 (right panel), based on CCLM (a, b), AgMERRA (c, d), CHIRPS (e, f), and EWEMBI (g, h). For the two definitions, see Table 2. Areas without significant rainfall, in which no rainy season is simulated, are given in gray. AgMERRA = Agricultural Modern-Era Retrospective Analysis for Research and Applications; CCLM = COnsortium for Small-scale MOdelling in CLimate Mode; CHIRPS = Climate Hazards Group Infrared Precipitation with Stations; EWEMBI = E2OBS and WFDEI applied to ERA-Interim data Merged and Bias-corrected for Inter-Sectoral Impact Model Intercomparison Project; ORS = onset of the rainy season.

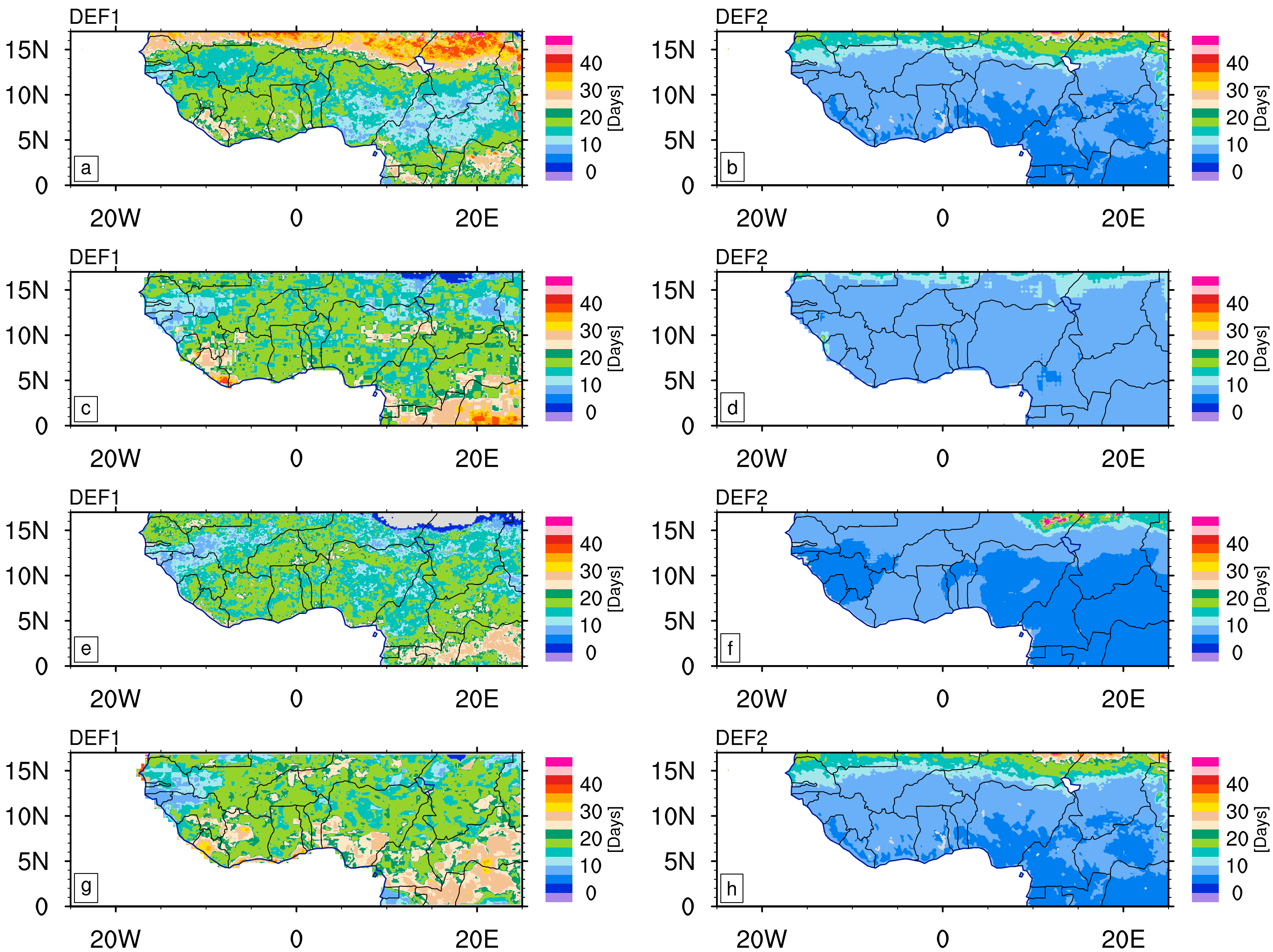

Figure 6. Standard deviation of mean onset date (ORS) for the period 1981–2010 according to DEF1 (left panel) and DEF2 (right panel), based on CCLM (a, b), AgMERRA (c, d), CHIRPS (e, f), and EWEMBI (g, h). AgMERRA = Agricultural Modern-Era Retrospective Analysis for Research and Applications; CCLM = COnsortium for Small-scale MOdelling in CLimate Mode; CHIRPS = Climate Hazards Group Infrared Precipitation with Stations; EWEMBI = E2OBS and WFDEI applied to ERA-Interim data Merged and Bias-corrected for Inter-Sectoral Impact Model Intercomparison Project; ORS = onset of the rainy season.

rainfall amounts (Table 3). It can be seen that CCLM exhibits a late ORS date with a median around DOY 120 (for both definitions), while it is about DOY 70 in all observations for DEF2 over the Guinea region. Moreover, CCLM shows early ORS dates around DOY 150 and DOY 170 in the observations in DEF2 over the Sahel region. The range of the ORS distribution in the Sahel region is smaller in DEF2 (DOY 120–225) compared to DEF1 (DOY 120–275).

Figure 8 shows the mean date of the CRS for the period 1981–2010 using the two definitions (see Table 2). The CRS usually progresses from September to mid-October. Remarkable differences are found in the CRS dates between the different observations by applying DEF1 but a good agreement by using DEF2. For example, AgMERRA and CHIRPS show similar patterns in DEF1 with early areal average mean CRS dates (DOY 240–250) compared to EWEMBI, and CCLM differs from them in providing a more realistic patterns. As expected, the Sahel region with high precipitation uncertainty shows the earliest CRS among the regions. With exceptions of AgMERRA and CHIRPS for DEF1, the observed CRS lies around DOY 240–260 (28 August to 27 September), followed by the Savanna region around DOY 250–280 (17 September to 7 October), and the Guinea region around DOY 340–350 (6–16 December) for both definitions. In comparison to DEF2, DEF1 shows a more scattered pattern for AgMERRA and CHIRPS. This is caused by the thresholds used in DEF1

10.1029/2018JD028536

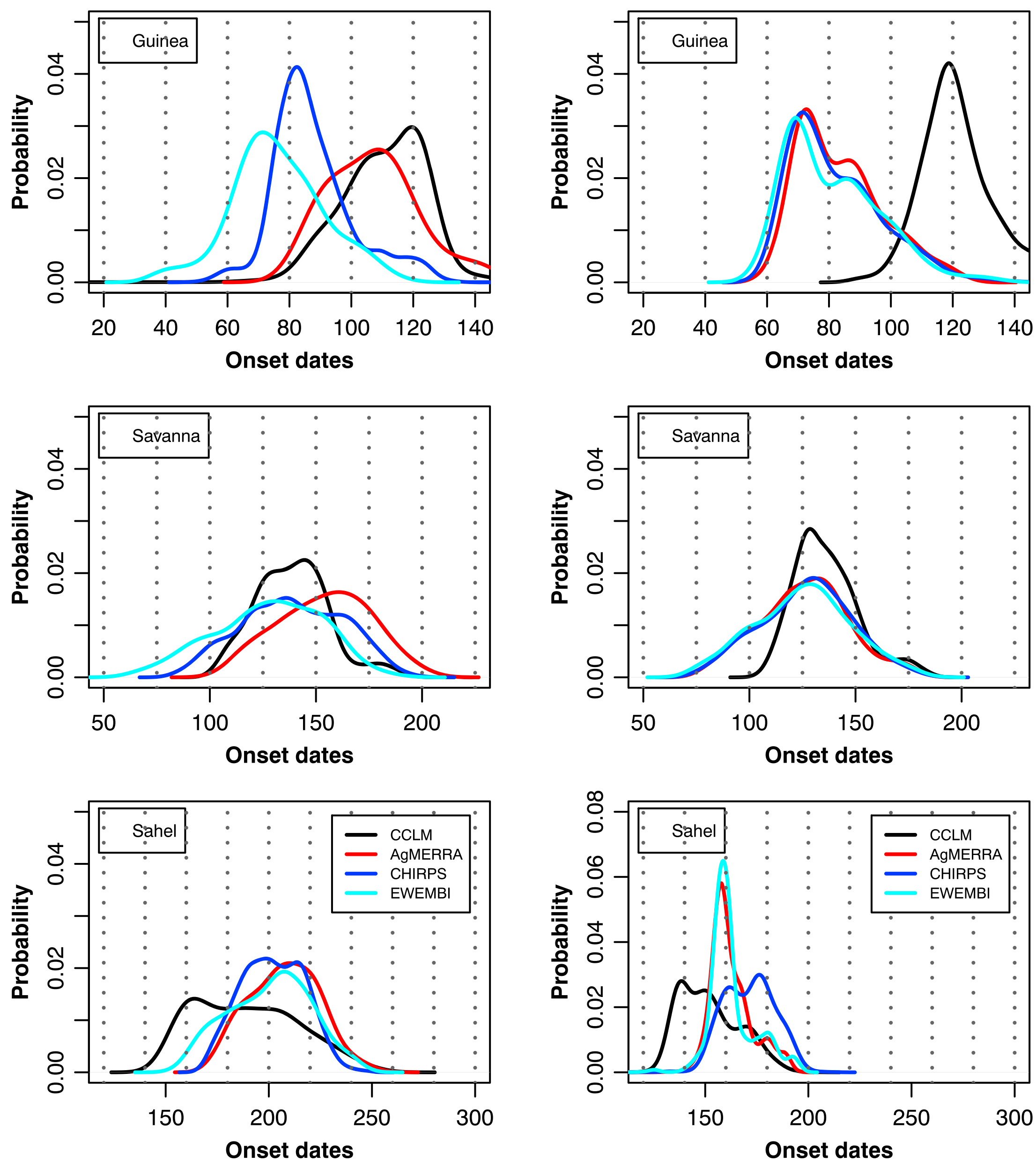

Figure 7. Probability density function of areal mean onset date (ORS) according to DEF1 (left panel) and DEF2 (right panel) for the period 1981–2010 over the Guinea, the Savanna, and the Sahel regions. AgMERRA = Agricultural Modern-Era Retrospective Analysis for Research and Applications; CCLM = COnsortium for Small-scale MOdelling in CLimate Mode; CHIRPS = Climate Hazards Group Infrared Precipitation with Stations; EWEMBI = E2OBS and WFDEI applied to ERA-Interim data Merged and Bias-corrected for Inter-Sectoral Impact Model Intercomparison Project; ORS = onset of the rainy season.

(compared to the smooth accumulation function applied in DEF2). The apparent stripes patterns in AgMERRA are presumably related to the merging of model results and observations from satellite and stations.

In line with the ORS, a reasonable estimate of the CRS allows the derivation of the LRS, which is illustrated in Figure 9. The LRS is a crucial information for the selection of crop varieties and sequences (Kowal & Knabe, 1972). Similar to the CRS, the LRS increases from the Sahel region (DOY 50–100) to the Guinea region (DOY 300–340). This can be explained by the migration of the Intertropical Convergence Zone, which is controlling the monsoonal flux of humid maritime air masses onto the continent. The LRS is generally shorter over the coastal regions in AgMERRA and CHIRPS, respectively, due to their earlier CRS dates (Figure 8). In the Sahel region, the LRS is slightly shorter in CCLM for DEF2 (DOY 274) than for DEF1 (DOY 325). For DEF1, the LRS differences between CCLM and the observations is larger than for DEF2. The maximum average difference is

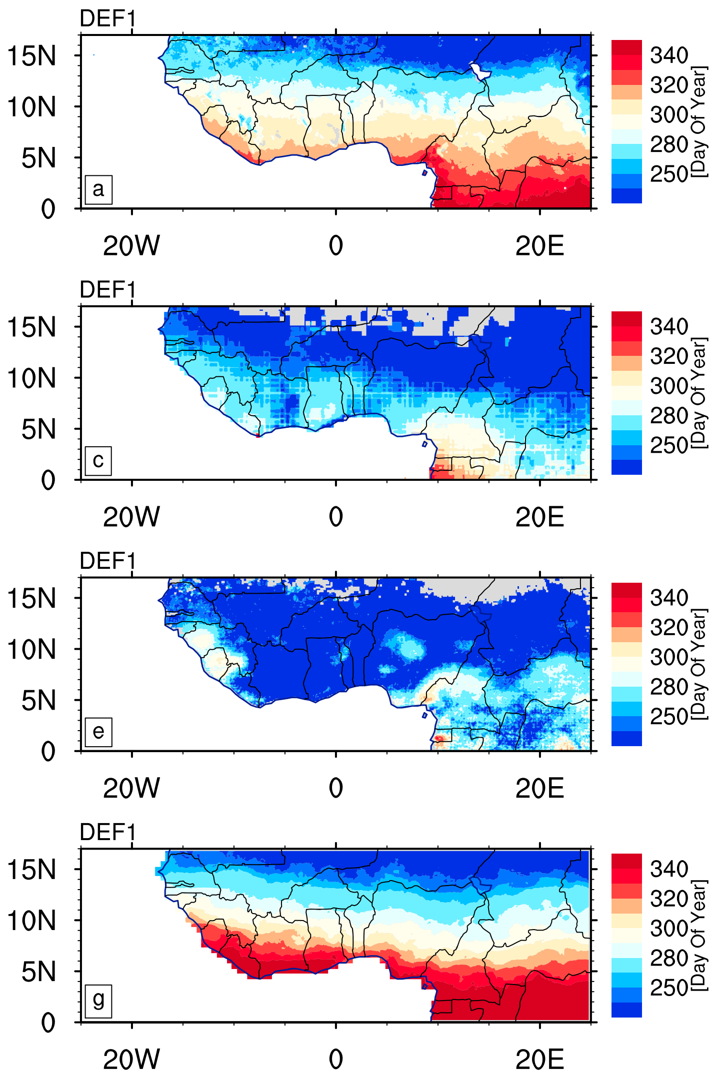

Figure 8. Mean cessation date (CRS) for the period 1981–2010 according to definition DEF1 (left panel) and DEF2 (right panel), based on CCLM (a, b), AgMERRA (c, d), CHIRPS (e, f), and EWEMBI (g, h). For the two definitions, see Table 2. Areas without significant rainfall, in which no rainy season is simulated, are given in gray. AgMERRA = Agricultural Modern-Era Retrospective Analysis for Research and Applications; CCLM = COnsortium for Small-scale MOdelling in CLimate Mode; CHIRPS = Climate Hazards Group Infrared Precipitation with Stations; EWEMBI = E2OBS and WFDEI applied to ERA-Interim data Merged and Bias-corrected for Inter-Sectoral Impact Model Intercomparison Project; CRS = cessation of the rainy season.

20 days in DEF1, while it is 15 days in DEF2 (not shown). Differences in the estimation of the LRS are related to deficiencies in the estimation of the CRS. This is in agreement with previous studies (Mugalavai et al., 2008; Oladipo & Kyari, 1993; Sivakumar, 1988).

Climatological variables such as temperature and precipitation are essential information for agricultural production. For instance, the accumulated temperature, which can be expressed as GDD is known to be crucial for crop development. It is therefore used to model the timing when crops reach particular growing stages. Figure 10 presents the GDD over West Africa for the period 1981–2010, calculated for each grid cell using the daily minimum and maximum temperature from the CCLM simulations and observations from AgMERRA and EWEMBI. For maize, sorghum, and pearl millet, a base temperature (T_{base}) of 10, 25, and 23°C is assumed, respectively.

The observations show variations between 1657 and 2185°C for maize, 214 to 781°C for sorghum, and 305 to 770°C for pearl millet over the region. Differences between the three crops are due to differences in their T_{base} and MVP only. For maize, there are relatively small differences (maximum up to 17%) between the spatial patterns of CCLM and the observations. In the case of sorghum, there are substantial differences and the

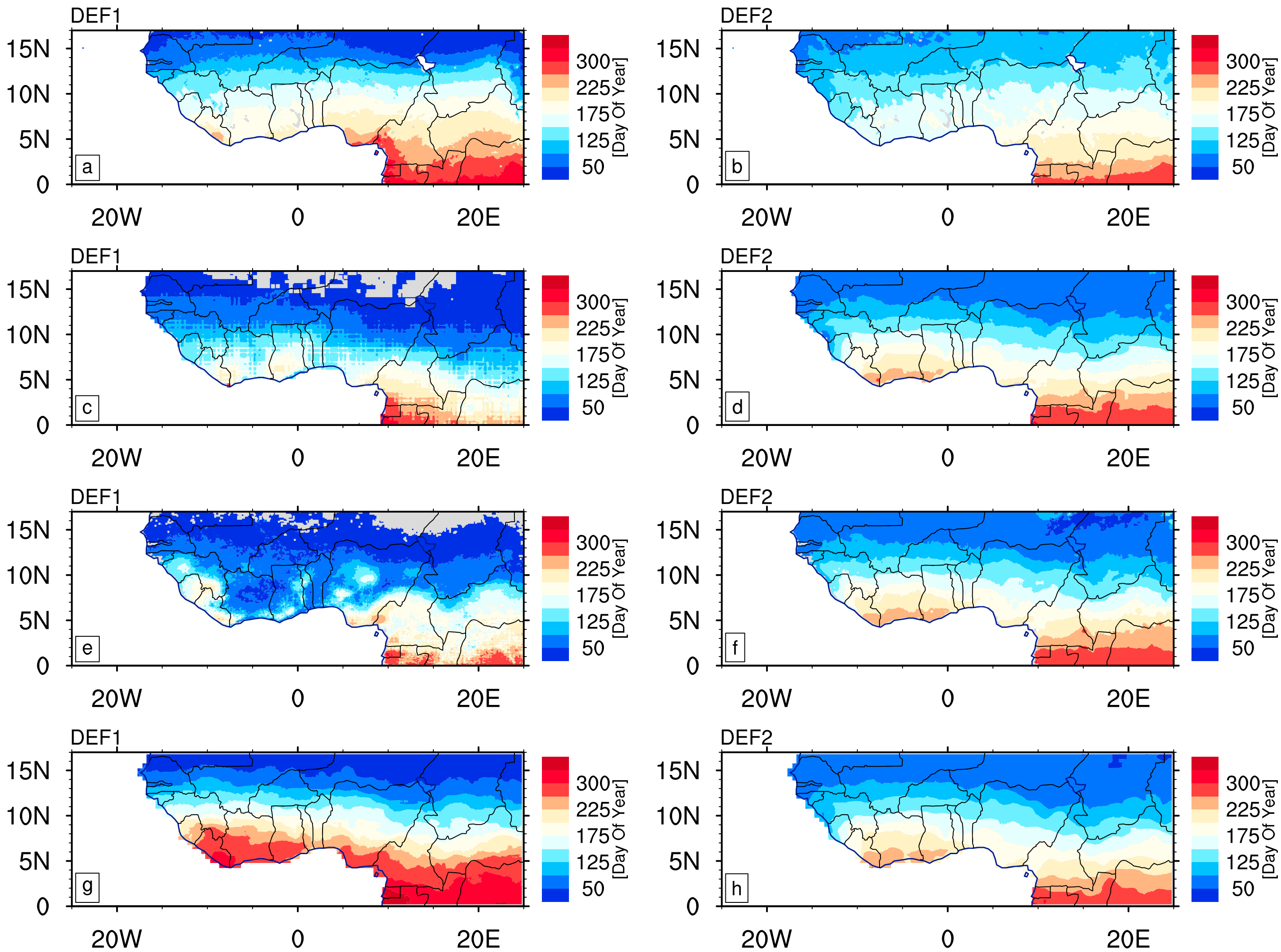

Figure 9. Mean length of the rainy season (LRS) for the period 1981–2010 according to definition DEF1 (left panel) and DEF2 (right panel), based on CCLM (a, b), AgMERRA (c, d), CHIRPS (e, f), and EWEMBI (g, h). For the two definitions, see Table 2. Areas without significant rainfall, in which no rainy season is simulated, are given in gray. AgMERRA = Agricultural Modern-Era Retrospective Analysis for Research and Applications; CCLM = COnsortium for Small-scale MOdelling in CLimate Mode; CHIRPS = Climate Hazards Group Infrared Precipitation with Stations; EWEMBI = E2OBS and WFDEI applied to ERA-Interim data Merged and Bias-corrected for Inter-Sectoral Impact Model Intercomparison Project; LRS = length of the rainy season.

range of GDD variability is higher (respectively, slightly less than 235°C over the Guinea region, 238°C over the Savanna region, and 328°C over the Sahel region). In particular for pearl millet, the CCLM generally produces lower values of GDD with differences up to 65% for AgMERRA and up to 69% for EWEMBI over the Sahel region.

In order to achieve a sustainable crop field based on an efficient water resource management, reliable estimations of WAV are needed. The WAV (Figure 11) for the three crops follows the general north-south gradient of precipitations patterns (see supporting information Figure S2 and Table 3). Nearly all observations show similar WAV patterns across the region with maximum WAV values reaching more than 350 mm for maize and sorghum, and between 180 to 270 mm for pearl millet. In general, there is a good agreement between CCLM and the three observations with some regions of disagreement. The greatest wetting in CCLM compared to AgMERRA and CHIRPS is in the Sahel region (especially northern Senegal and Mali) and the Guinean Highlands (from central Guinea Bissau through northern Sierra Leone and Liberia to western Ivory Coast) with differences between 185 and 450 mm. CCLM shows the best agreement with EWEMBI. Here the differences are reaching values of about 58 mm for maize, 70 mm for sorghum, and 60 mm for pearl millet. For the Guinea region, the difference between the simulation and the observations do not exceed 150 mm (30%) for pearl millet, 120 mm (16%) for sorghum, and 100 mm (16%) for maize.

10.1029/2018JD028536

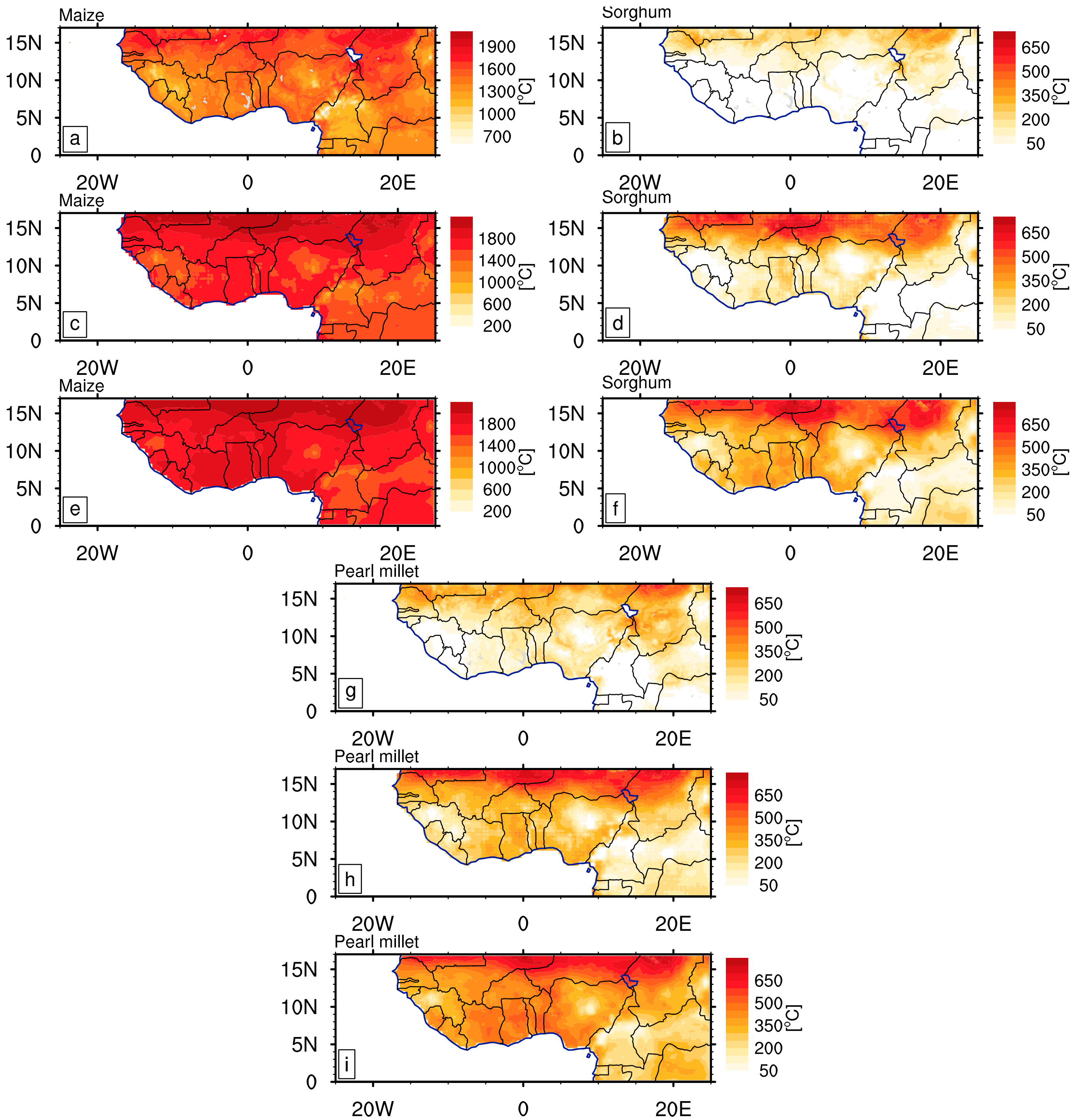

Figure 10. Mean accumulated growing degree days (°C) according to DEF1 for the period 1981–2010, based on CCLM (a, b, g), AgMERRA (c, d, h), and EWEMBI (e, f, i) during the minimum vegetation period for maize, sorghum, and pearl millet. AgMERRA = Agricultural Modern-Era Retrospective Analysis for Research and Applications; CCLM = COnsortium for Small-scale MOdelling in CLimate Mode; EWEMBI = E2OBS and WFDEI applied to ERA-Interim data Merged and Bias-corrected for Inter-Sectoral Impact Model Intercomparison Project.

10.1029/2018JD028536

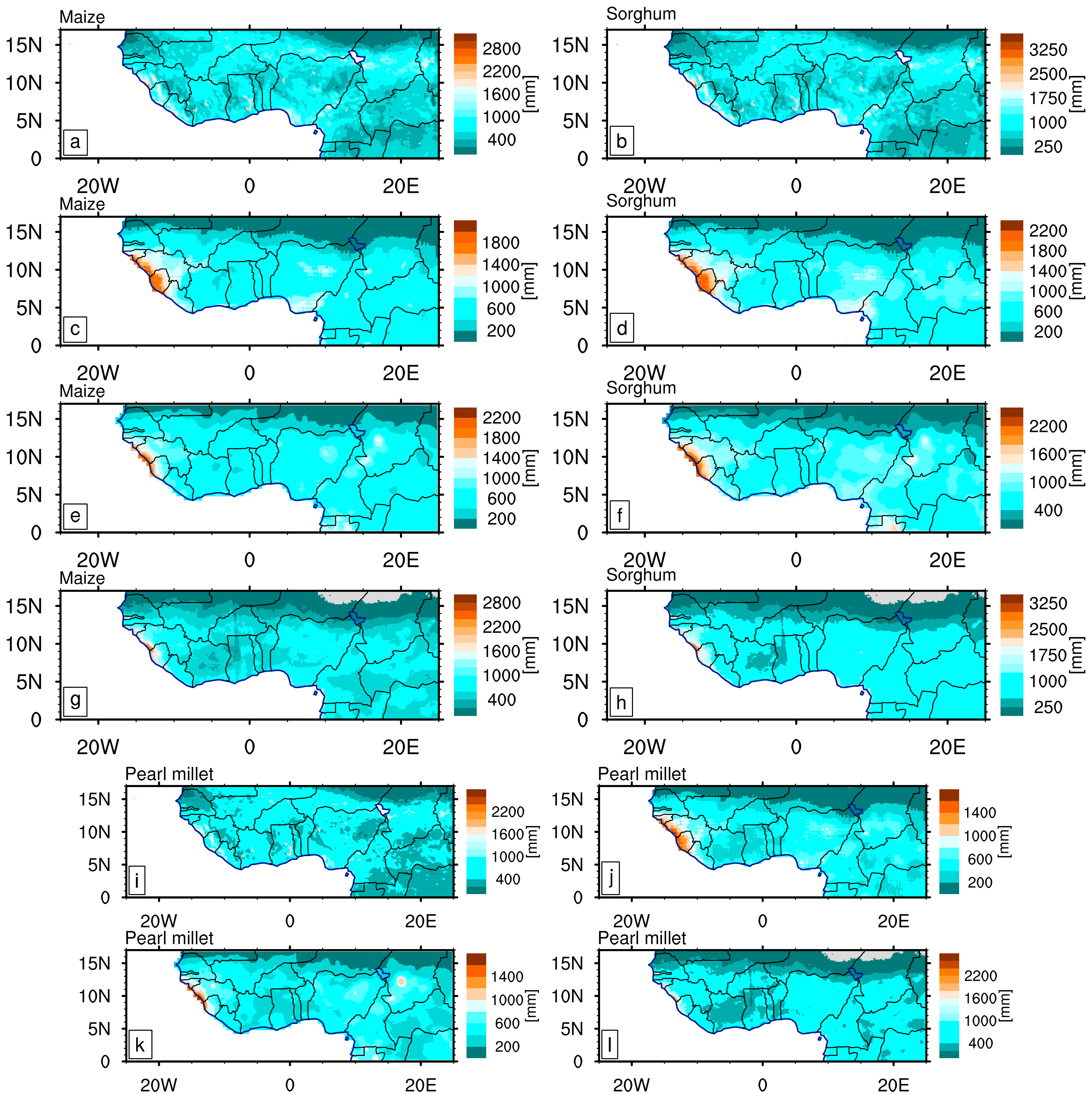

Figure 11. Mean water availability (mm) for the period 1981–2010 according to DEF1, based on CCLM (a, b, i), AgMERRA (c, d, j), CHIRPS (e, f, k), and EWEMBI (g, h, l) during the minimum vegetation period for maize, sorghum, and pearl millet. AgMERRA = Agricultural Modern-Era Retrospective Analysis for Research and Applications; CCLM = COnsortium for Small-scale MOdelling in CLimate Mode; CHIRPS = Climate Hazards Group Infrared Precipitation with Stations; EWEMBI = E2OBS and WFDEI applied to ERA-Interim data Merged and Bias-corrected for Inter-Sectoral Impact Model Intercomparison Project.

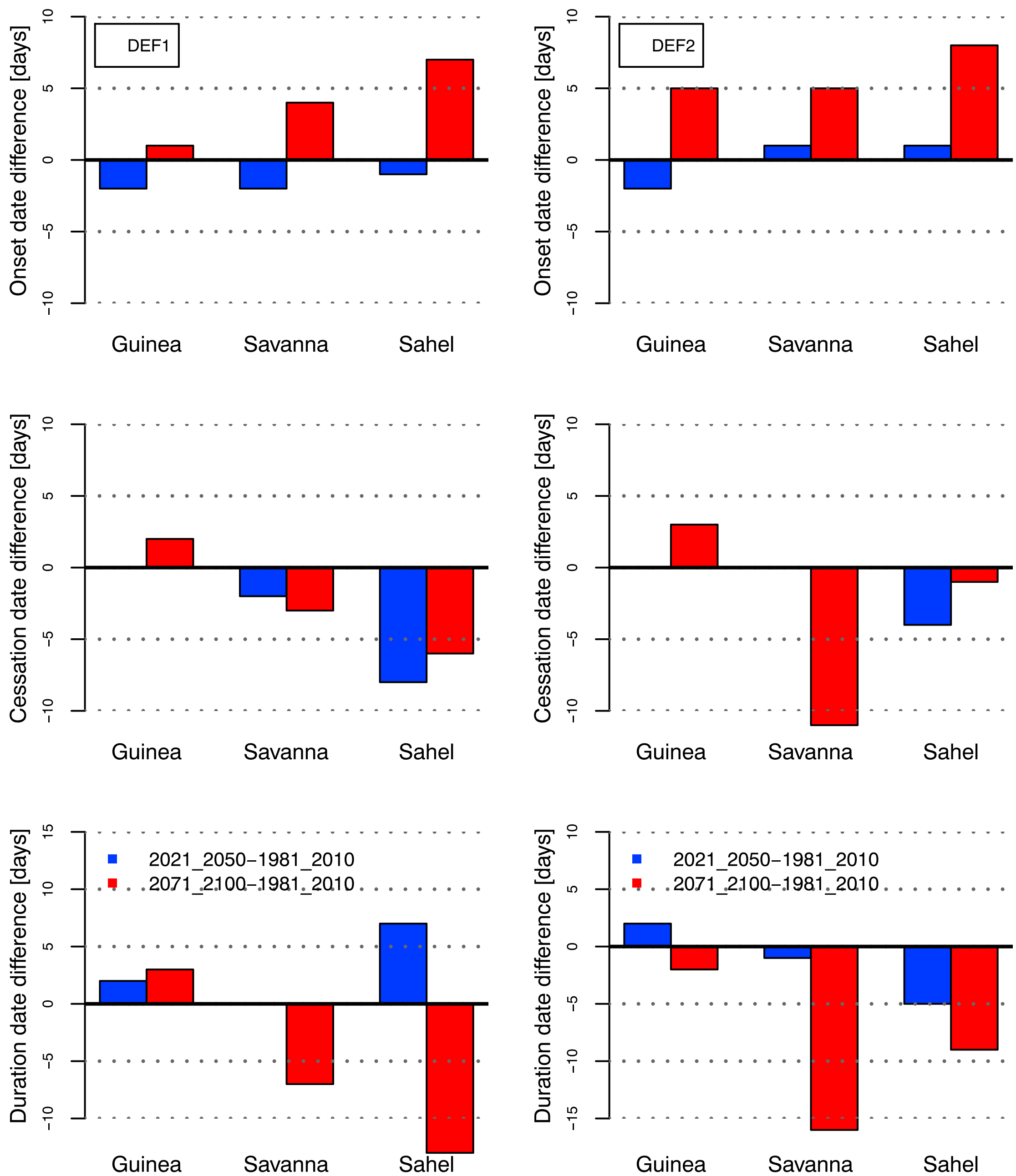

Figure 12. Areal mean ORS, CRS, and LRS differences (future minus past dates) according to DEF1 (left panel) and DEF2 (right panel) over the Guinea, the Savanna, and the Sahel regions. AgMERRA = Agricultural Modern-Era Retrospective Analysis for Research and Applications; CCLM = COnsortium for Small-scale MOdelling in CLimate Mode; CHIRPS = Climate Hazards Group Infrared Precipitation with Stations; EWEMBI = E2OBS and WFDEI applied to ERA-Interim data Merged and Bias-corrected for Inter-Sectoral Impact Model Intercomparison Project.

Despite the differences in the spatial patterns between the three observations and CCLM, it is noted that model and observations exhibit a similar trend for maize, sorghum, and pearl millet between 1981 and 2010 (Figures 10 and 11). The poor representation of GDD and the WAV in CCLM over the Sahel region is probably due to the underestimation of temperature and the overestimation of precipitation in this region. The ability of CCLM in reproducing the observed patterns of the selected indicators provides additional information and justification regarding their future projections. A comparison between the expected future and the present provides an avenue to estimate how the critical indices for agricultural production might develop for the future.

10.1029/2018JD028536

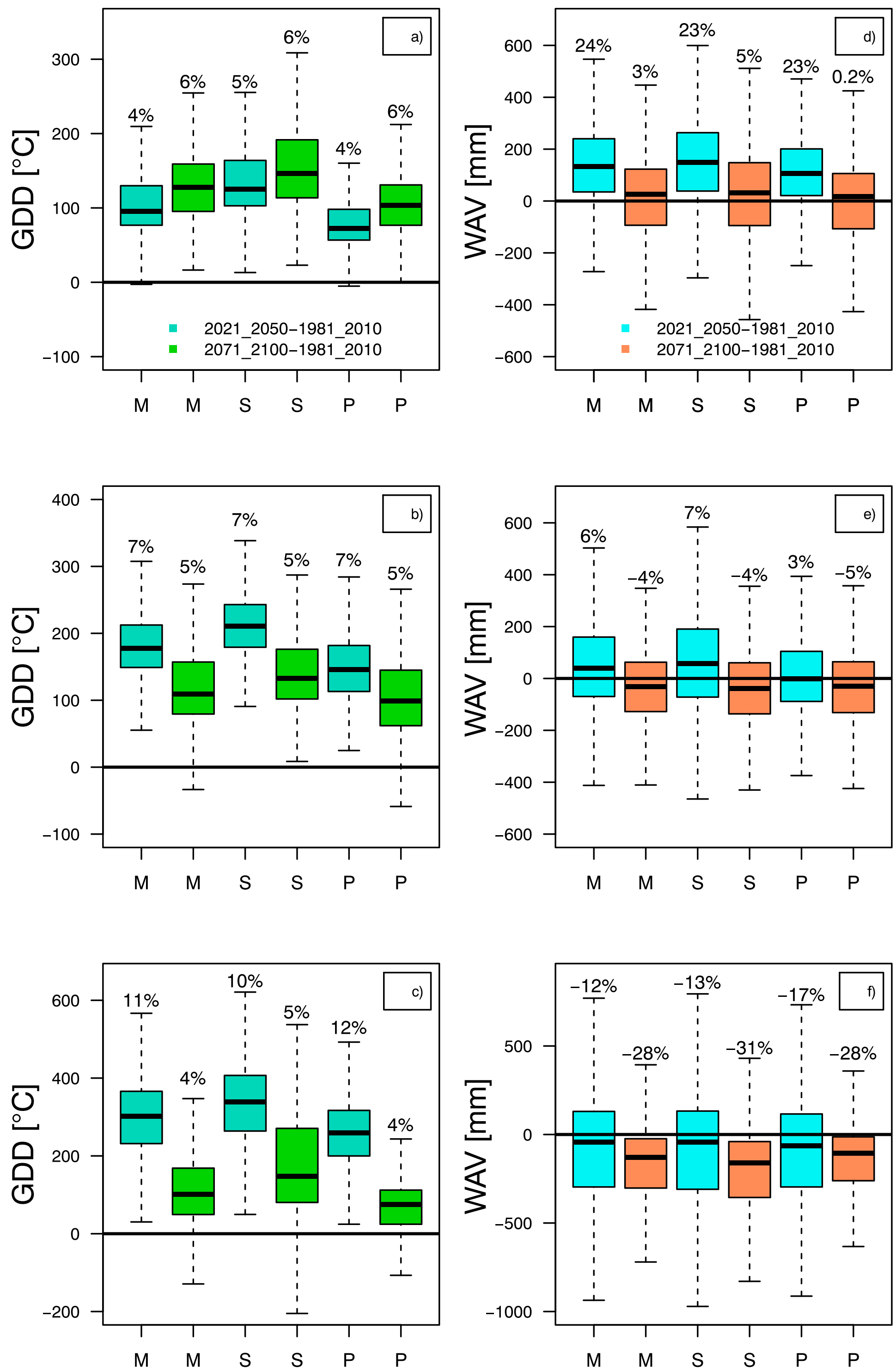

Figure 13. Projected future changes in mean GDD (left panel) and WAV (right panel) for 2021–2050 and 2071–2100 relative to 1981–2010 according to definition DEF1. (a, d) for the Guinea, (b, e) for the Savanna, and (c, f) for the Sahel regions. The bold black horizontal lines mark the median, the thin horizontal lines span the interquartile range (25% to 75% percentiles) and the vertical dashed lines represent extremes. Numbers above each box express the projected changes for each crop (M = Maize, S = Sorghum, and P = Pearl millet) in the two future periods. GDD = growing degree days; WAV = water availability.

10.1029/2018JD028536

Table 4
Mean Onset Days/Date for the Period 1981–2010 According to DEF1 and DEF2, Based on CCLM, AgMERRA, CHIRPS, and EWEMBI Over the Guinea, the Savanna, and the Sahel Regions

Index	DEF1		DEF2	
	Days	Date	Days	Date
		Guinea		
CCLM	110 ± 16	20 April	121 ± 5	30 April
AgMERRA	106 ± 18	16 April	83 ± 7	23 March
CHIRPS	86 ± 16	27 March	82 ± 5	22 March
EWEMBI	76 ± 21	13 March	81 ± 3	21 March
		Savanna		
CCLM	138 ± 15	18 May	136 ± 6	15 May
AgMERRA	154 ± 17	3 June	126 ± 6	5 May
CHIRPS	139 ± 15	19 May	127 ± 5	6 May
EWEMBI	127 ± 17	8 May	125 ± 4	4 May
		Sahel		
CCLM	189 ± 19	8 July	152 ± 13	31 May
AgMERRA	207 ± 14	26 July	162 ± 10	10 June
CHIRPS	201 ± 14	20 July	171 ± 30	19 June
EWEMBI	200 ± 16	19 July	162 ± 11	10 June

Note. AgMERRA = Agricultural Modern-Era Retrospective Analysis for Research and Applications; CHIRPS = Climate Hazards Group Infrared Precipitation with Stations; EWEMBI = E2OBS and WFDEI applied to ERA-Interim data Merged and Bias-corrected for Inter-Sectoral Impact Model Intercomparison Project; CCLM = COnsortium for Small-scale MOdelling in CLimate Mode.

3.3. Expected Impact of Climate Change

To estimate the change in ORS, CRS, and LRS variability due to increasing greenhouse gases as assumed in RCP4.5 scenario, results of CCLM climate projections were analyzed. Figure 12 illustrates the expected areal mean differences between the future (2021–2050 and 2071–2100) and historical climate dates for the ORS, the CRS, and the LRS for the different regions. The spatial patterns for the two definitions (DEF1 and DEF2) are similar (not shown). Across West Africa, a delay of 1 to 6 days in DEF2 is expected, in contrast to DEF1 with a delay of 1 to 29 days for the period 2021–2050 (not shown). There is an earlier start of the ORS by up to 4 days in DEF1 and by up to 6 days in DEF2 in the period 2071–2100. However, the results differ by regions: There are no significant changes over the Guinea region with an advanced mean ORS of up to 2 days during the 2021–2050 (maximum of 20 days, not shown) and a mean ORS delay by up to 7 days for the period 2071–2100 (maximum up to 27 days, not shown). The highest mean changes in the ORS dates are predicted over the Sahel region, especially for the period 2071–2100 with a delay of up to 7 days. Past modeling studies over the semiarid region of West Africa (Biasutti & Sobel, 2009; Jung & Kunstmann, 2007) suggested a delay of the ORS of about 1 month for the period 2030–2039 (compared to the period 1991–2000). For the same period, however, the CRS as well as the total rainfall amount is expected to remain more or less unchanged.

For the CRS, the results indicate a delay of about 2 and 8 days, and for the LRS a delay of about 7 and 15 days for the period 2021–2050 and 2071–2100 over the Savanna and the Sahel regions, respectively. For the Guinea region, almost no more change is found for these periods, suggesting normal conditions compared to the period 1981–2010.

In summary, for the periods 2021–2050 and 2071–2100, CCLM predicts no changes to the ORS for the Guinea region and only small changes for the Savanna and the Sahel regions compared to 1981–2010. For all regions, the CRS is predicted to occur mostly earlier by up to 15 days. The simulated future change (not shown) also indicates a decrease of up to 20% in the mean daily precipitation for both periods. With almost no change in the ORS, the earlier occurrence of the CRS translates into a shorter LRS by up to 15 days in the Sahel region.

There is large consensus that in West Africa, one of the major climate change impacts will be on rainfall. This changing climate will affect the ORS, the CRS, and the LRS of growing seasons, particularly in semiarid areas where yields from rainfed agriculture could be reduced by up to 20–50% by 2050 (Sarr, 2012). Accordingly,

Table 5
Changes of Statistics of GDD and WAV for the Three Different Crops Across the Study Region for 2021–2050 and 2071–2100 Relative to the Present Period 1981–2010 (%)

			Guinea		Savanna		Sahel	
Variables		Description	2021–2050	2071–2100	2021–2050	2071–2100	2021–2050	2071–2100
Maize	GDD	Average	6	4	8	5	12	5
		Minimum	7	8	−9	−10	4	4
		Maximum	8	5	9	2	14	10
Sorghum	GDD	Average	6	4	7	5	11	8
		Minimum	7	7	7	6	10	5
		Maximum	7	4	9	3	13	9
Pearl millet	GDD	Average	6	4	8	6	13	4
		Minimum	6	8	14	5	12	4
		Maximum	9	7	2	2	14	10
Maize	WAV	Average	16	−2	12	−6	−6	−27
		Minimum	**67**	−30	**116**	−19	7	**−77**
		Maximum	4	−12	20	11	−0.4	−18
Sorghum	WAV	Average	16	2	12	−5	−6	−27
		Minimum	**53.8**	−31	**123**	−23	7	**−77**
		Maximum	8.3	−8	22	10	9	−18
Pearl millet	WAV	Average	12	−10	4	−11	−10	−23
		Minimum	−10	−48	**63**	−25	−4	**−77**
		Maximum	−1.4	−13	28	17	−2	−18

Note. Values larger than ±50% are bolded. GDD = growing degree days; WAV = water availability.

the climate change signal of the GDD and the WAV is represented by the box-and-whisker plots and is shown as differences 2021–2050 minus 1981–2010, and 2071–2100 minus 1981–2010 in Figure 13. Averaged over entire whole West Africa, the increase in GDD Figures 13a–13c is mostly associated with the increase in the mean temperature (not shown). The future mean GDD increases by 167 to 230°C for 2021–2050 and between 96 and 150°C for 2071–2100 compared to the historical period (1981–2010). Mean projected changes are characterized by an increase in GDD by up to 11%, 10%, and 12% for maize, sorghum, and pearl millet in 2021–2050 but to a lesser extent in 2071–2100 between 4% and 6% for maize, sorghum, and pearl millet, respectively. The largest differences are projected for the period 2021–2050 in the Savanna and in the Sahel regions for the period 2071–2100. The regional mean difference over the Guinea region ranges up to 109, 138, and 84°C in 2021–2050 and up to 135, 160, and 109°C in 2071–2070 for maize, sorghum, and pearl millet, respectively. In summary, the Sahel region is expected to see a higher GDD up to 287, 321, and 249°C for the future, that is, an increase by approximately 12% compared to the historical period. Previous studies by Salack et al. (2015); Ruiz Castillo and Gaitán Ospina (2016) found that under climate change, higher temperatures will result in a more rapid accumulation of GDD and therefore a reduction of certain crop development phases and the growth cycle. As such, the increased temperatures and CO_2 concentrations will have negative impacts on crop yields for food-insecure regions such as West Africa. Lobell et al. (2008) estimate that climate change has a >95% chance to harm crop production in absence of adaptation with a decrease by up to 10% in crop yields.

The WAV distributions (Figures 13d–13f) reveal major differences between the two time slices and only minor differences between the crops types. In general, for West Africa, the spatial distribution of the mean difference between the simulated near-future 2021–2050 and the historical period 1981–2010 indicate moderate increase (up to 32 mm [5.3%], 37 mm [5.1%], and 11 mm [0.2%] for maize, sorghum, and pearl millet, respectively; not shown). Meanwhile, for the distant future 2071–2100, the WAV decreases for all crops by 62 mm (−10%) for maize, 75 mm (−10.5%) for sorghum, and 58 mm (−11.8%) for pearl millet on average (not shown). With respect to the different regions, the WAV is expected to increase less in the Guinea region than in the Savanna region and is expected to decrease in the Sahel region for both periods. A closer look on the regional differences for the present and the period 2021–2050 shows increases by 24% and 7% in the Guinea and the Savanna regions and a decrease by −17% in the Sahel region. In contrast to the period 2021–2050, the WAV decreases for all crops for the period 2071–2100 by −31% and −5% in the Sahel and the Savanna regions and increases by 5% in the Guinea region. Previous crop yield simulations in West Africa showed the effect of rainfall and temperature changes on mean crop yield of sorghum and millet (Sultan et al., 2013). They found that mean crop yields decreased mainly as to a response an increase in temperature. When warming exceeded 2°C, mean crop yields were always found to decrease significantly. Rainfall changes were only able to modulate the magnitude of this negative impact.

The mean percentage changes in the average, minimum, and maximum GDD and WAV for 2021–2050 and 2071–2100 with respect to the historical period 1981–2010 are estimated according to the definition in Table 5 for the different regions. Under the investigated RCP4.5 climate change scenario, this leads to an average increase of 13% in the GDD. In contrast, the WAV shows an increase by around 16% for 2021–2050 and an decreased of up to −27% in 2071–2100, respectively. Minimum and maximum values increase more substantially for the period 2021–2050 than for the period 2071–2100 for all regions. For the GDD, the largest increase occurs over the Sahel region and changes in the maximum are a slightly more pronounced than changes in means for all crops. Changes in GDD are mainly due to the shift of the whole distribution to warmer values, and our results seem to confirm those from (Heinzeller et al., 2018), which suggest an increase of 1.5°C at the Coast of Guinea and of up to 3°C in the Sahel region under RCP4.5. For the maximum change in WAV, the largest increase is found over the Savanna region of up to 28% and changes in minimum exceed changes in means considerably, especially for sorghum. In addition, changes in WAV are also associated with changes in different important rainfall-related factors for agriculture implications such as the ORS and an early CRS, especially for millet, sorghum, and maize (Salack et al., 2011; Sivakumar, 1992; Sultan et al., 2005). For example, Lobell et al. (2011) estimated that climate change from 1980 to 2008 has already reduced global production of maize by 3.8% and wheat by 5.5%, relative to a counterfactual without climate change. At the same time, Knox et al. (2012) reported a projected mean change in yield of −5% (maize), −5% (sorghum), and −10% (millet) by 2050 across Africa. However, despite the increase in the GDD and decrease in WAV indices, maize, sorghum, and pearl millet might be successfully grown with careful consideration. Sultan et al. (2013) conclude that the probability of a yield reduction appears to be greater in the Sudanian region (southern Senegal, Mali, Burkina Faso, northern Togo, and Benin), because of an exacerbated sensitivity to temperature changes compared to the Sahelian region (Niger, Mali, northern parts of Senegal, and Burkina Faso), where crop yields are more sensitive to rainfall change.

4. Summary and Conclusions

Our study focuses on the effects of current and expected future climate conditions on precipitation- and temperature-related agroclimatic indices over West Africa. The high-resolution CCLM RCM is validated in terms of representing crucial agroclimatic indices based on precipitation and temperature across West Africa against different observation data. The new data set provides a potentially valuable source for (local) climate impact studies. As such, spatially explicit climate data may help farmers to meet strategic cropping decisions such as changes of crops (and varieties) and adaptations of cropping calendars. Aggregated results as often provided for the agroclimatic zones are limited value for local climate impact studies only.

Under current (1981–2010) and two future climate conditions (2021–2050 and 2071–2100), the ORS, CRS, and LRS as well as the GDD and WAV are derived based on the plant physiological requirements of maize, sorghum, and pearl millet.

For the baseline period, the results demonstrate that the mean regional ORS and CRS dates (resulting in the LRS) largely depend on the selected approach (DEF1 and DEF2) and the underlying observation data. Independent of the applied approach, biases are highest for the Guinean region, followed by the Sahel and the Savanna regions. Overall, CCLM produces negative biases of GDD for sorghum over the Sahel region (ranging from 64% to 69%) compared to the observations, while the WAV agree well with the observations over all regions.

For the future time slice 2021–2050 (2071–2100), the ORS and CRS dates are expected to occur later (earlier) by about 1 week than in the present climate. Both future periods also suggest an increase in GDD and WAV, except for the Sahel region, where WAV is expected to decreased up to 10% in 2021–2050 and by up to 24% in 2071–2100 due to the increased temperatures. It is likely that such projected increases in mean temperature will accelerate the crop development, resulting in shorter crop durations and reduced time to accumulate biomass and reduced yield at the end.

The conclusions drawn in this study are based on one future scenario and one regional-global climate model only. Multimodel multiscenario ensembles are suspected to be more robust and possibly less affected by uncertainties, compared to the results of our study. However, due to the lack of current means for quantifying the errors in long-term climate projections the additional computational costs for such multimodel multiscenario ensembles are still questionable. Recently, an ensemble of multimodel intercomparison project consisting of a large quantity of different GCMs and RCMs has been analyzed to assess and quantity uncertainties from different sources, that is, the driving GCM, the future scenario, as well as the internal variability and spatial resolution of the RCM. Despite of a lacking full factorial design of the different uncertainty sources and their relative contribution to the total uncertainty range, they concluded the GCM to be main contributor of the uncertainty range. The emission scenario, at least for the near future, did not lead to strong uncertainties (Fernández et al., 2018). Moreover, it is critically noted that despite of the high horizontal resolution used in our study, noticeable biases still persist, which could affect our results, particularly in parts of the Guinea and the Sahel regions. More detailed discussions about model deficiencies leading to the poor model representations of large-scale mechanisms are given in Dieng et al. (2017). In order to retain the physical consistency between precipitation and temperature given by the RCM simulations, we decided to abstain from any postprocessing bias correction. Existing state-of-the-art bias correction routines, applied for precipitation and temperature separately might introduce additional biases, possibly exceeding those coming from the RCM itself. Multivariate bias correction methods may help to overcome these limitations and will be subject of future investigations. To derive suitable climate change adaptation strategies, these biases must be considered, even when the relative changes of the climate projections (compared to the baseline simulations) are assumed to be important information for long-term agricultural planning. Differences between high-resolution model results and the different observation data sets are also due to data scarcity and, related to that, interpolation issues, which underpin the need for an improved station network in this region.

This study is assumed to improve the number of assessment risks of climate change with respect to maize, sorghum, and pearl millet and other agricultural systems across different agroclimatic zones in West Africa.

Acknowledgments
The authors gratefully acknowledge financial support of the German Federal Ministry of Science and Education (BMBF), through the West Africa Science Service Center on Climate Change and Adapted Land Use (WASCAL) project (grant number:01LG1202C1), and the Steinbuch Centre for Computing (SCC) for providing computing resources at the ForHLR I supercomputer.
The data can be accessed under http://doi.org/10.5281/zenodo.1255882. We thank Zenodo for hosting the model data.

References

Abiodun, B. J., Adeyewa, Z. D., Oguntunde, P. G., Salami, A. T., & Ajayi, V. O. (2012). Modeling the impacts of reforestation on future climate in West Africa. *Theoretical and Applied Climatology*, *110*(1), 77–96. https://doi.org/10.1007/s00704-012-0614-1

Alagarswamy, G., & Ritchie, J. (1991). Phasic development in CERES-Sorghum model. In T. Hodges (Ed.), *Predicting crop phenology* (pp. 143–152). Boca Raton, FL: CRC Press.

Alhassane, A., Salack, S., Ly, M., Lona, I., Traoré, S. B., & Sarr, B. (2013). Évolution des risques agroclimatiques associés aux tendances récentes du régime pluviométrique en afrique de l'ouest soudano-sahélienne. *Science et Changements Planétaires/Sécheresse*, *24*(4), 282–293. https://doi.org/10.1684/sec.2013.0400

Biasutti, M., & Sobel, A. (2009). Delayed Sahel rainfall and global seasonal cycle in a warmer climate. *Geophysical Research Letters*, *36*, L23707. https://doi.org/10.1029/2009GL041303

Calton, B., Schellekens, J., & Martinez-de la Torre, A. (2016). Water resource reanalysis v1: Data access and model verification results. *Earth System Science Data*, *36*(23). https://doi.org/10.5281/zenodo.57760

Carew, R., Smith, E. G., & Grant, C. (2009). Factors influencing wheat yield and variability: Evidence from Manitoba, Canada. *Journal of Agricultural and Applied Economics*, *41*(3), 625–639. https://doi.org/10.1017/S1074070800003114

Crafts-Brandner, S. J., & Salvucci, M. E. (2002). Sensitivity of photosynthesis in a C4 plant, maize, to heat stress. *Plant Physiology*, *129*(4), 1773–1780. https://doi.org/10.1104/pp.002170

Dee, D., Uppala, S., Simmons, A., Berrisford, P., Poli, P., Kobayashi, S., et al. (2011). The ERA-interim reanalysis: Configuration and performance of the data assimilation system. *Quarterly Journal of the Royal Meteorological*, *137*(656), 553–597. https://doi.org/10.1002/qj.828

Del Rio, A., & Brent, M. S. (2014). Agricultural adaptation to climate change in the Sahel: A review of fifteen crops cultivated in the Sahel. USAID.

Diallo, I., Giorgi, F., Deme, A., Tall, M., Mariotti, L., & Gaye, A. T. (2016). Projected changes of summer monsoon extremes and hydroclimatic regimes over West Africa for the twenty-first century. *Climate Dynamics*, *47*(12), 3931–3954. https://doi.org/10.1007/s00382-016-3052-4

Dieng, D., Smiatek, G., Bliefernicht, J., Heinzeller, D., Sarr, A., Gaye, A., & Kunstmann, H. (2017). Evaluation of the COSMO-CLM high-resolution climate simulations over West Africa. *Journal of Geophysical Research: Atmospheres*, *122*, 1437–1455. https://doi.org/10.1002/2016JD025457

Doms, G., Förstner, J., Heise, E., Herzog, H., Mironov, D., Raschendorfer, M., et al. (2011). A description of the nonhydrostatic regional COSMO model. Part II: Physical parameterization. *Deutscher Wetterdienst*, *154*, 161.

Dosio, A., & Panitz, H.-J. (2016). Climate change projections for CORDEX-Africa with COSMO-CLM regional climate model and differences with the driving global climate models. *Climate Dynamics*, *46*(5-6), 1599–1625. https://doi.org/10.1007/s00382-015-2664-4

Dosio, A., Panitz, H.-J., Schubert-Frisius, M., & Lüthi, D. (2015). Dynamical downscaling of CMIP5 global circulation models over CORDEX-Africa with COSMO-CLM: Evaluation over the present climate and analysis of the added value. *Climate Dynamics*, *44*(9–10), 2637–2661. https://doi.org/10.1007/s00382-014-2262-x

Dupuis, I., & Dumas, C. (1990). Influence of temperature stress on in vitro fertilization and heat shock protein synthesis in maize (Zea mays L.) reproductive tissues. *Plant Physiology*, *94*(2), 665–670. https://doi.org/10.1104/pp.94.2.665

FAO (2016). La situation mondiale de l'alimentation et de l'agriculture 2016 (SOFA): Changement climatique, agriculture et sécurité alimentaire, Organisation des Nations Unies pour l'alimentation et l'agriculture, doi:978-92-5-209374-9

Fernández, J., Frías, M. D., Cabos, W. D., Cofiño, A. S., Domínguez, M., Fita, L., et al. (2018). Consistency of climate change projections from multiple global and regional model intercomparison projects. *Climate Dynamics*. https://doi.org/10.1007/s00382-018-4181-8

Funk, C. C., Peterson, P. J., Landsfeld, M. F., Pedreros, D. H., Verdin, J. P., Rowland, J. D., et al. (2014). A quasi global precipitation time series for drought monitoring. *U.S. Geological Survey*, *832*, 4. https://doi.org/110.3133/ds832

Heinzeller, D., Dieng, D., Smiatek, G., Olusegun, C., Klein, C., Hamann, I., et al. (2018). The WASCAL high-resolution regional climate simulation ensemble for West Africa: Concept, dissemination and assessment. *Earth System Science Data (ESSD)*, *10*, 815–835. https://doi.org/10.5194/essd-10-815-2018

Herms, D. (2004). Using degree-days and plant phenology to predict pest activity. In V. Krischik & J. Davidson (Eds.), *IPM (integrated pest management) of midwest landscapes* (Vol. 316, pp. 49–59). St. Paul, MN: Minnesota Agricultural Experiment Station Publication SB-07645.

Herrero, M., & Johnson, R. (1980). High temperature stress and pollen viability of maize. *Crop Science*, *6*, 796–800. https://doi.org/10.2135/cropsci1980.0011183X002000060030x

Ilesanmi, O. (1972). Empirical formulation of onset, advance, and retreat of rainfall in Nigeria. *Journal of Tropical Geography*, *34*(JUN), 17–24.

Jung, G., & Kunstmann, H. (2007). High-resolution regional climate modeling for the Volta region of West Africa. *Journal of Geophysical Research*, *112*, D23108. https://doi.org/10.1029

Juszczak, R., Leśny, J., & Olejnik, J. (2008). Cumulative degree-days values as an element of agrometeorological forecast of the Wielkopolska region internet based agrometeorological information service (WISIA). *Acta Agrophysica*, *12*, 409–426.

Kim, H.-J., Wang, B., & Ding, Q. (2008). The global monsoon variability simulated by CMIP3 coupled climate models. *Journal of Climate*, *21*(20), 5271–5294. https://doi.org/10.1175/2008JCLI2041.1

Knox, J., Hess, T., Daccache, A., & Wheeler, T. (2012). Climate change impacts on crop productivity in Africa and South Asia. *Environmental Research Letters*, *7*(3), 034032.

Kowal, J., & Knabe, D. (1972). *An agroclimatological Atlas of the Northern States of Nigeria*. Samaru-Zaria, Nigeria: The Ahmadu Bello University Press.

Laux, P., Jäckel, G., Tingem, R. M., & Kunstmann, H. (2010). Impact of climate change on agricultural productivity under rainfed conditions in Cameroon-A method to improve attainable crop yields by planting date adaptations. *Agricultural and Forest Meteorology*, *150*(9), 1258–1271. https://doi.org/10.1016/j.agrformet.2010.05.008

Laux, P., Kunstmann, H., & Bárdossy, A. (2008). Predicting the regional onset of the rainy season in West Africa. *International Journal of Climatology*, *28*(3), 329–342. https://doi.org/10.1002/joc.1542

Laux, P., Wagner, S., Wagner, A., Jacobeit, J., Bárdossy, A., & Kunstmann, H. (2009). Modelling daily precipitation features in the Volta Basin of West Africa. *International Journal of Climatology*, *29*(7), 937–954. https://doi.org/10.1002/joc.1852

Lobell, D. B., Burke, M. B., Tebaldi, C., Mastrandrea, M. D., Falcon, W. P., & Naylor, R. L. (2008). Prioritizing climate change adaptation needs for food security in 2030. *Science*, *319*(5863), 607–610. https://doi.org/10.1126/science.1152339

Lobell, D. B., Schlenker, W., & Roberts, J. C. (2011). Climate trends and global crop production since 1980. *Science*, *333*(6042), 616–620. https://doi.org/10.1126/science.1204531

Maiti, R. K. (1996). *Sorghum science*. Lebanon, NH: Science Publishers.

Miller, P., Lanier, W., & Brandt, S. (2001). Using growing degree days to predict plant stages, Ag/Extension Communications Coordinator, Communications Services Montana State University-Bozeman, Bozeman, MO.

Mishra, A., Hansen, J. W., Dingkuhn, M., Baron, C., Traoré, S. B., Ndiaye, O., & Ward, M. N. (2008). Sorghum yield prediction from seasonal rainfall forecasts in Burkina Faso. *Agricultural and Forest Meteorology*, *148*(11), 1798–1814. https://doi.org/10.1016/j.agrformet.2008.06.007

Morel, R. (1992). Atlas agroclimatique des pays de la zone du CILSS. Cooperation française.

Mounkaila, M. S., Abiodun, B. J., & Omotosho, J. (2015). Assessing the capability of CORDEX models in simulating onset of rainfall in West Africa. *Theoretical and Applied Climatology*, *119*(1–2), 255. https://doi.org/10.1007/s00704-014-1104-4

Mugalavai, E. M., Kipkorir, E. C., Raes, D., & Rao, M. S. (2008). Analysis of rainfall onset, cessation and length of growing season for western Kenya. *Agricultural and Forest Meteorology*, *148*(6), 1123–1135. https://doi.org/10.1016/j.agrformet.2008.02.013

Odekunle, T. (2004). Rainfall and the length of the growing season in Nigeria. *International Journal of Climatology*, *24*(4), 467–479. https://doi.org/10.1002/joc.1012

Odekunle, T. (2006). Determining rainy season onset and retreat over Nigeria from precipitation amount and number of rainy days. *Theoretical and Applied Climatology*, *83*(1), 193–201. https://doi.org/10.1007/s00704-005-0166-8

Oladipo, E., & Kyari, J. (1993). Fluctuations in the onset, termination and length of the growing season in Northern Nigeria. *Theoretical and Applied Climatology*, *47*(4), 241–250. https://doi.org/10.1007/BF00866245

Olaniran, O. (1983). The onset of the rains and the start of the growing season in Nigeria. *Nigerian Geographical Journal*, *26*(1), 81–88.

Omotosho, J. B. (1990). Onset of thunderstorms and precipitation over northern Nigeria. *International Journal of Climatology*, *10*(8), 849–860. https://doi.org/10.1002/joc.3370100807

Omotosho, J., & Abiodun, B. J. (2007). A numerical study of moisture build-up and rainfall over West Africa. *Meteorological Applications*, *14*(3), 209–225. https://doi.org/10.1002/met.11

Ong, C., & Monteith, J. (1985). Response of pearl millet to light and temperature. *Field Crop Research*, *11*, 141–160. https://doi.org/10.1016/0378-4290(85)90098-X

Parthasarathi, T., Velu, G., & Jeyakumar, P. (2013). Impact of crop heat units on growth and developmental physiology of future crop production: A review. *Research & Reviews: A Journal of Crop Science and Technology*, *2*, 1–11.

Prasad, P. V., Boote, K. J., & Allen, L. H. (2006). Adverse high temperature effects on pollen viability, seed-set, seed yield and harvest index of grain-sorghum [Sorghum bicolor (L.) Moench] are more severe at elevated carbon dioxide due to higher tissue temperatures. *Agricultural and Forest Meteorology*, *139*(3), 237–251. https://doi.org/10.1016/j.agrformet.2006.07.003

Ramel, R., Gallée, H., & Messager, C. (2006). On the northward shift of the West African monsoon. *Climate Dynamics*, *26*(4), 429–440. https://doi.org/10.1007/s00382-005-0093-5

Ruane, A. C., Goldberg, R., & Chryssanthacopoulos, J. (2015). Climate forcing datasets for agricultural modeling: Merged products for gap-filling and historical climate series estimation. *Agricultural and Forest Meteorology*, *200*, 233–248. https://doi.org/10.1016/j.agrformet.2014.09.016

Ruiz Castillo, N., & Gaitán Ospina, C. F. (2016). Projecting future change in growing degree days for winter wheat. *Agriculture*, *6*(3), 47. https://doi.org/10.3390/agriculture6030047

Salack, S., Muller, B., & Gaye, A. T. (2011). Rain-based factors of high agricultural impacts over Senegal. Part I: Integration of local to sub-regional trends and variability. *Theoretical and Applied Climatology*, *106*(1–2), 1–22. https://doi.org/10.1007/s00704-011-0414-z

Salack, S., Sarr, B., Sangare, S. K., Ly, M., Sanda, I. S., & Kunstmann, H. (2015). Crop-climate ensemble scenarios to improve risk assessment and resilience in the semi-arid regions of West Africa. *Climate Research*, *65*, 107–121. https://doi.org/10.3354/cr01282

Sarr, B. (2012). Present and future climate change in the semi-arid region of West Africa: A crucial input for practical adaptation in agriculture. *Atmosphere Science Letter*, *13*(2), 108–112. https://doi.org/10.1002/asl.368

Schoper, J. B., Lambert, R. J., Vasilas, B. L., & Westgate, M. E. (1987). Plant factors controlling seed set in maize the influence of silk, pollen, and ear-leaf water status and tassel heat treatment at pollination. *Plant Physiology*, *83*(1), 121–125. https://doi.org/10.1104/pp.83.1.121

Sijikumar, S., Roucou, P., & Fontaine, B. (2006). Monsoon onset over Sudan-Sahel: Simulation by the regional scale model MM5. *Geophysical Research Letters*, *33*, L03814. https://doi.org/10.1029/2005GL024819

Sivakumar, M. (1988). Predicting rainy season potential from the onset of rains in southern Sahelian and Sudanian climatic zones of West Africa. *Agricultural and Forest Meteorology*, *42*(4), 295–305. https://doi.org/10.1016/0168-1923(88)90039-1

Sivakumar, M. (1992). Empirical analysis of dry-spells for agricultural applications in West Africa. *Journal of Climate*, *5*, 532–539. https://doi.org/10.1175/1520-0442(1992)005<0532:EAODSF>2.0.CO;2

Sivakumar, M. (1998). Climate variability and food vulnerability. *Global Change Newsletter (IGBP)*, *35*, 14–17.

Sivakumar, M., Maidoukia, A., & Stern, R. (1993). Agroclimatology of West Africa: Niger, vol. 5, International Crops Research Institute for the Semi-Arid Tropics (ICRISAT).

Stern, R., Dennett, M., & Garbutt, D. (1981). The start of the rains in West Africa. *International Journal of Climatology*, *1*(1), 59–68. https://doi.org/10.1002/joc.3370010107

Stevens, B., Giorgetta, M., Esch, M., Mauritsen, T., Crueger, T., Rast, S., et al. (2013). Atmospheric component of the MPI-M Earth System Model: ECHAM6. *Journal of Advances in Modeling Earth Systems*, *5*(2), 146–172. https://doi.org/10.1002/jame.20015

Stewart, I. (1986). Response farming: A scientific approach to ending starvation and alleviating poverty in drought zones of Africa. In *Proceedings, African Agricultural Development conference: Technology, Ecology and Society*.

Sultan, B., Baron, C., Dingkuhn, M., Sarr, B., & Janicot, S. (2005). Agricultural impacts of large-scale variability of the West African monsoon. *Agricultural and Forest Meteorology*, *128*(1), 93–110. https://doi.org/10.1016/j.agrformet.2004.08.005

Sultan, B., Roudier, P., Quirion, P., Alhassane, A., Muller, B., Dingkuhn, M., et al. (2013). Assessing climate change impacts on sorghum and millet yields in the Sudanian and Sahelian savannas of West Africa. *Environmental Research Letters*, *8*(1), 014040. https://doi.org/1748-9326/8/i=1/a=014040

Syed, F., Yoo, J., Körnich, H., & Kucharski, F. (2010). Are intraseasonal summer rainfall events micro monsoon onsets over the western edge of the South-Asian monsoon? *Atmospheric Research*, *98*, 341–346. https://doi.org/10.1016/j.atmosres.2010.07.006

Sylla, M. B., Giorgi, F., Pal, J. S., Gibba, P., Kebe, I., & Nikiema, M. (2015). Projected changes in the annual cycle of high-intensity precipitation events over West Africa for the late twenty-first century. *Journal of Climate*, *28*(16), 6475–6488. https://doi.org/10.1175/JCLI-D-14-00854.1

Traoré, S. B., Carlson, R. E., Pilcher, C. D., & Rice, M. E. (2000). Bt and non-Bt maize growth and development as affected by temperature and drought stress. *Agronomy Journal*, *92*(5), 1027–1035.

UN (2017). World Population Prospects, The 2017 Revision: Key Findings and Advance Tables, United Nations Population Division.

Vanvyve, E., Hall, N., Messager, C., Leroux, S., & Van Ypersele, J.-P. (2008). Internal variability in a regional climate model over West Africa. *Climate Dynamics*, *30*(2), 191–202. https://doi.org/10.1007/s00382-007-0281-6

Vellinga, M., Arribas, A., & Graham, R. (2013). Seasonal forecasts for regional onset of the West African monsoon. *Climate Dynamics*, *40*(11–12), 3047–3070. https://doi.org/10.1007/s00382-012-1520-z

Waongo, M., Laux, P., & Kunstmann, H. (2015). Adaptation to climate change: The impacts of optimized planting dates on attainable maize yields under rainfed conditions in Burkina Faso. *Agricultural and Forest Meteorology*, *205*, 23–39. https://doi.org/10.1016/j.agrformet.2015.02.006

Waongo, M., Laux, P., Traoré, S. B., Sanon, M., & Kunstmann, H. (2014). A crop model and fuzzy rule based approach for optimizing maize planting dates in Burkina Faso, West Africa. *Journal of Applied Meteorology and Climatology*, *53*(3), 598–613. https://doi.org/10.1175/JAMC-D-13-0116.1

Weedon, G. P., Balsamo, G., Bellouin, N., Gomes, S., Best, M. J., & Viterbo, P. (2014). The WFDEI meteorological forcing data set: WATCH forcing data methodology applied to ERA-Interim reanalysis data. *Water Resources Research*, *50*, 7505–7514. https://doi.org/10.1002/2014WR015638

Wheeler, T., Challinor, A., Osborne, T., & Slingo, J. (2007). *Development of a Combined Crop and Climate Forecasting System for Seasonal to Decadal Predictions* (pp. 31–40). Berlin: Springer.

Willmott, C. J., & Matsuura, K. (1995). Smart interpolation of annually averaged air temperature in the United States. *Journal of Applied Meteorology*, *34*(12), 2577–2586. https://doi.org/10.1175/1520-0450(1995)034h2577:SIOAAAi2.0.CO;2